Journal of Human Evolution 183 (2023) 103414

Contents lists available at ScienceDirect

Journal of Human Evolution

journal homepage: www.elsevier.com/locate/jhevol

The stratigraphy and formation of Middle Stone Age deposits in Cave 1B, Klasies River Main site, South Africa, with implications for the context, age, and cultural association of the KRM 41815/SAM-AP 6222 human mandible

Peter Morrissey [a, *], Susan M. Mentzer [b], Sarah Wurz [a, c]

[a] School of Geography, Archaeology and Environmental Studies, University of the Witwatersrand, Johannesburg, South Africa
[b] Senckenberg Centre for Human Evolution and Palaeoenvironment, Institute for Archaeological Sciences, Department of Geosciences, Eberhard Karls Universität Tübingen, Tübingen, Germany
[c] SFF Centre for Early Sapiens Behaviour (SapienCE), University of Bergen, Bergen, Norway

ARTICLE INFO

Article history:
Received 9 April 2023
Accepted 12 July 2023
Available online 1 September 2023

Keywords:
Klasies River
Archaeological micromorphology
Middle Stone Age
Site formation
Archaeological stratigraphy

ABSTRACT

Cave 1B, in the Klasies River Main site complex (KRM), is best known for the recovery of the KRM 41815/SAM-AP 6222 human mandible. After initial skepticism over the modernity of this specimen, it is accepted that the mix of archaic and modern traits it displays is characteristic of early *Homo sapiens* individuals. Different authors have associated this specimen with the Middle Stone Age (MSA) I and II/Mossel Bay cultural phases, but the published data do not allow an unambiguous attribution. KRM 41815's frequent use in studies of the evolution of the human mandible, and its well-developed chin, makes clarifying its age and context important objectives. The field and micromorphology observations presented here provide greater insight into the stratigraphy and formation of the sequence exposed in the PP38 excavation. There are three major divisions: the basal Light Brown Sand (LBS) Member (not excavated), the Rubble Sand (RS) Member (MSA I), and the Shell and Sand Dark Carbonized (SASDC) Submember (MSA II). Cultural stratigraphy based on lithic artifacts remains the only way to make secure (but broad) temporal correlations with the rest of the site complex. This investigation shows that a range of anthropogenic, geogenic, and biogenic processes contributed to the deposition and post-depositional alteration of the identified microfacies. Short depositional hiatuses are reasonably common, and a significant hiatus was identified between the RS and SASDC. The impact of post-depositional processes on the RS is significant, with anthropogenic deposits poorly preserved. In comparison, the SASDC is dominated by hearths contained within deposits rich in reworked anthropogenic materials known as carbonized partings. Small shell disposal features are also present. The distribution of these anthropogenic features suggests continuity in the management of space throughout the MSA II occupations, from before 110 ka. New stratigraphic correlations indicate that KRM 41815 is unambiguously associated with the MSA I. Therefore, it predates 110 ka, with a lower age limit potentially in Marine Isotope Stage 6.

1. Introduction

Archaeological assemblages excavated from caves and rock shelters along South Africa's southern and Western Cape coast have contributed significantly to understanding the development of modern human cognition during the Middle Stone Age (MSA) from Marine Isotope Stage (MIS) 6 onwards (McBrearty and Brooks, 2000; Henshilwood and Marean, 2003; Wadley, 2015). These finds have provided insight into innovative behaviors including the earliest known use (and later, the oldest known intensive use) of marine food resources, and early symbolic practices (e.g., Henshilwood et al., 2004, 2009, 2011; Marean et al., 2007; Marean, 2014, 2016; Niespolo et al., 2021; Tribolo et al., 2022; Wurz et al., 2022). However, in contrast to the rich assemblages of artifacts and faunal remains, these sites have yielded few human fossil specimens (Grine, 2016). Relatively large Late Pleistocene human

* Corresponding author.
E-mail address: Peter.Morrissey@students.wits.ac.za (P. Morrissey).

https://doi.org/10.1016/j.jhevol.2023.103414

fossil assemblages have been recovered only from Die Kelders Cave 1 (DK1) and Klasies River Main site (KRM). The DK1 assemblage comprises 30 specimens which are mostly teeth, along with two finger bones, a single thumb bone, and a mandible fragment (Grine, 2000; Grine et al., 2017a). The published sample from KRM includes more than 50 specimens,[1] which are predominantly cranial and mandibular (including teeth), with a far smaller proportion of postcranial bones (Singer and Wymer, 1982; Rightmire and Deacon, 1991, 2001; Grine et al., 1998, 2017b, 2020; Rightmire et al., 2006).

The specimens from KRM have played an important role in characterizing *Homo sapiens* anatomy during the Late Pleistocene (e.g., Bräuer, 1992; Smith, 1992; Grine, 2016; Bergmann et al., 2021; Grine et al., 2021). They display a mix of relatively archaic and more modern traits, and the size variation among the cranial and mandibular specimens is significant, perhaps reflecting far greater sexual dimorphism than is present in human populations today (e.g., Rightmire and Deacon, 1991; Smith, 1992; Bräuer and Singer, 1996; Lam et al., 1996; Rightmire, 2009; Royer et al., 2009). The morphology of the postcranial bones indicate that the represented individuals were relatively small-bodied, with similar proportions to Holocene hunter gatherers and modern Khoe-San people from the region (Cameron et al., 2021). This is argued to be the result of phenotypic adaptation to conditions in the Cape during these periods (Cameron et al., 2021).

Human fossils have been recovered across much of the site complex and from different parts of the sequence, but there are clear spatial and temporal patterns (Deacon, 2008; Grine et al., 2017b, 2020). Six confirmed specimens have been recovered from the MSA I deposits (Light Brown Sand [LBS] Member and Layer 37/ 'Rubble Brown Sand' ['RBS'][2] Member) in Cave 1 and at the Cave 1/ 1A boundary (Figs. 1 and 2), but more than 20 potential human fossils from Cave 1 were lost at some point between their excavation and Ronald Singer's analysis of the human fossil assemblage, meaning that they could not be confirmed as either human or animal. The MSA II/Mossel Bay deposits (Shell and Sand [SAS] Member) have proven to be far richer, with 40 confirmed specimens discovered in Cave 1 (34 of the 40) and in Cave 1A (the remaining six). A further five specimens come from the Upper Member in Cave 1A: one from the Howiesons Poort (HP), and four from the MSA III or post-HP. Only two specimens were recovered from Cave 1B (Singer and Wymer, 1982): the relatively robust partial mandible published as KRM 41815 (cataloged as SAM-AP 6222 at the Iziko Museums of South Africa in Cape Town), and an associated mandibular condyle, which disappeared at some point after Singer's analysis.

Cave 1 is clearly the richest area of the site complex for human fossils, with the MSA II–bearing SAS Member deposits yielding most of the sample (Deacon, 2008; Grine et al., 2017b, 2020). Abundant faunal remains have been recovered across the complex and throughout the sequence (Singer and Wymer, 1982; Van Pletzen-Vos et al., 2019; Reynard and Wurz, 2020), indicating that this pattern is not a product of variable preservation of bone in different areas. Dating of the sequence indicates that the fossil-bearing deposits span a significant period of time, from prior to MIS 5e up to ~43 ka (see recent reviews in Grine et al., 2017b; Wurz et al., 2018; Morrissey et al., 2022). Recent dating of speleothems associated with a hiatus in the basal SAS Member deposits in Cave 1 suggests that all specimens assigned to the MSA I and the oldest part of the MSA II (the SAS Lower [SASL] Submember or Singer and Wymer's Layer 17b) are older than 110 ka (Wurz et al., 2022).

Although the spatial and stratigraphic distribution of the human fossil specimens is generally well understood, the stratigraphic context of some has been the subject of debate. Hilary Deacon argued that many, if not all, of the human fossils assigned to the upper MSA II deposits in Cave 1 by John Wymer are actually associated with units near the base of the MSA II (Rightmire and Deacon, 1991; Deacon and Schuurman, 1992; Deacon, 2008). As the excavations were conducted at relatively low stratigraphic resolution, including in areas of Cave 1 where it was difficult to distinguish between deposits with similar properties and thus avoid mixing material between layers (Singer and Wymer, 1982), this is possible, but it cannot be proven or disproven with the evidence that is currently available. The cultural attribution of KRM 41815 has been particularly difficult to assess due to the lack of interconnecting deposits between Cave 1B and the rest of the KRM site complex and because there are no published absolute dates for the Cave 1B deposits. The mandible has been variously associated with the MSA I (e.g., Singer and Wymer, 1982; Deacon and Geleijnse, 1988; Grine et al., 2017b, 2021, 2023), MSA II (e.g., Deacon, 2008), and even the HP/MSA III (Binford, 1984; 1986b). A potential association with the HP/MSA III has subsequently been conclusively disproven (Deacon and Geleijnse, 1988; Thackeray, 1989, 1992; Wurz 2002), but the question of whether KRM 41815 dates to the MSA I or the MSA II has not been settled definitively due to a lack of published data (Morrissey et al., 2022).

The cultural attribution of KRM 41815—and thus, its age—is significant for understanding its temporal relationship to other specimens from Klasies. The mandible (Fig. 3) is fairly robust but is small in comparison to some other early *H. sapiens* mandibles and has a form broadly consistent with anatomically modern humans (Singer and Wymer, 1982; Smith, 1992; Lam et al., 1996; Bergmann et al., 2021). The corpus is described as "robust with bulging triangular mental protuberance" by Singer and Wymer (1982:146) who calculated a robusticity index of 48.93% at the right M_1. With the inclusion of the associated KRM 41820 mandibular condyle, the incomplete ramus appears to have been "massive" (Singer and Wymer, 1982:147). The preserved teeth are heavily worn, and there are indications of bone resorption (Singer and Wymer, 1982:146). This individual is estimated to have been the oldest at death of the KRM dental specimens and had suffered extreme hypercementosis (Grine et al., 2023). Of particular significance is the chin which, while somewhat controversial (e.g., Frayer et al., 1993; Wolpoff and Caspari, 1996), is the most strongly developed example of the mandibles at KRM (Singer and Wymer, 1982; Rightmire and Deacon, 1991; Bergmann et al., 2021; Grine et al., 2021). Whether it should be grouped with the MSA I or MSA II specimens has implications for assessing the overall anatomical characteristics of both groups of fossils and the breadth of variation in these populations. Given the paucity of *H. sapiens* fossils during this period (Grine, 2016), this also has significance beyond the site and the Cape coastal region.

The different areas excavated across the KRM site complex (Fig. 1) encompass a variety of depositional environments and human activity zones (Deacon and Geleijnse, 1988; Mentzer et al., 2014; Morrissey et al., 2022; Wurz et al., 2022). The resolution of excavation and recording and the amount of detail provided in descriptions of the stratigraphy of excavations have varied significantly between the coarser-scale excavations conducted in the late 1960s and the finer-scale work from 1984 onwards (Singer and Wymer, 1982; Deacon and Geleijnse, 1988; Wurz et al., 2018,

[1] Some unconfirmed specimens are missing from the museum collection, complicating a precise count.

[2] The 'RBS' in Cave 1 is a poorly understood stratigraphic entity in terms of its distribution and formation, and its relationship to both the LBS Member in Cave 1A and Wymer's Layer 37 in Caves 1 and 1A (Morrissey et al., 2022). The term is used throughout this paper for consistency with the existing literature, and because a re-evaluation of the 'RBS' is still in progress. Here it is used to refer explicitly to the deposits placed in this entity by Hilary Deacon (e.g., Deacon and Geleijnse, 1988: fig. 7; Rightmire and Deacon, 2001: fig. 2).

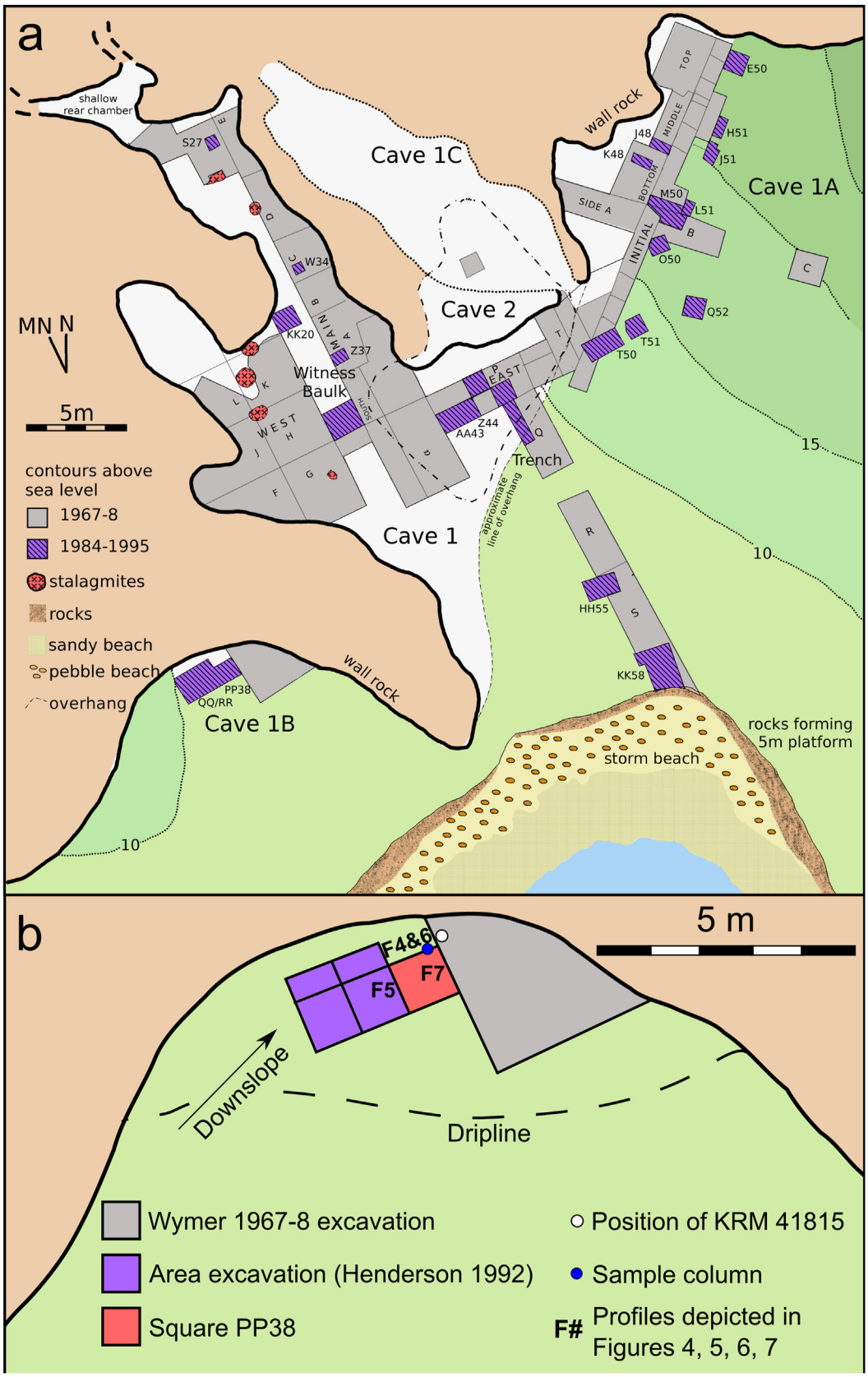

Figure 1. a) Map of the Klasies River Main site complex and b) Map of Cave 1B (after Deacon et al., 1986, Henderson, 1992; Wurz et al., 2018). (For interpretation of the references to color in this figure legend, the reader is referred to the web version of this article).

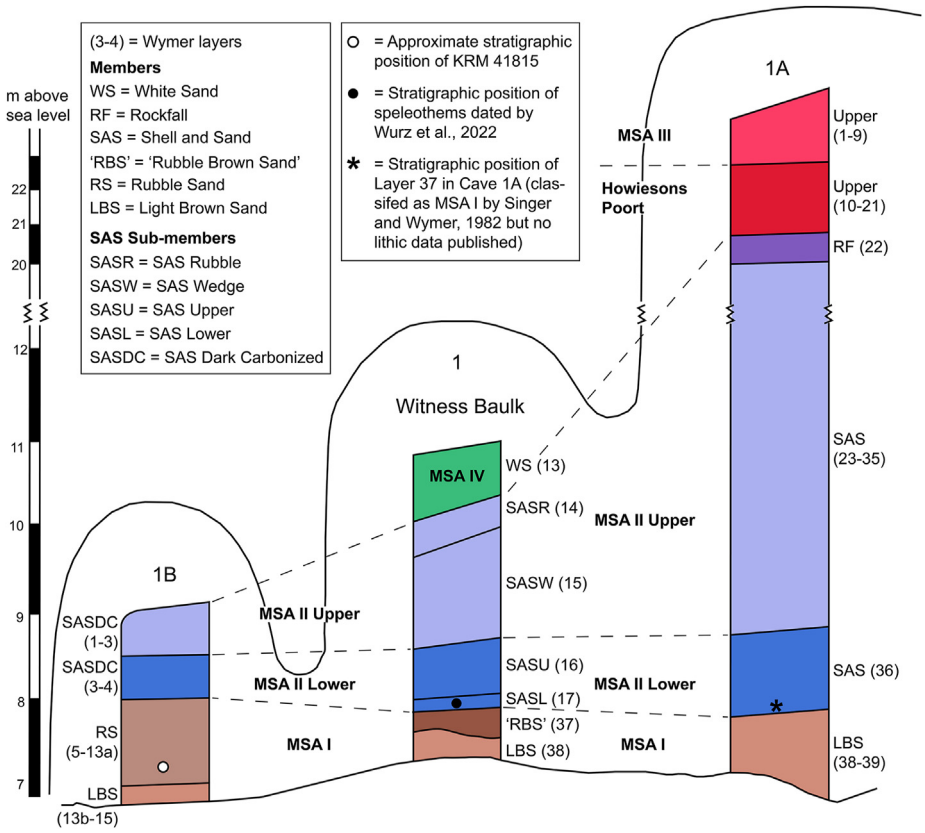

Figure 2. Simplified stratigraphy of the Middle Stone Age (MSA) deposits in Caves 1, 1A, and 1B at Klasies River Main site, showing the cultural stratigraphy, Wymer's excavation layers, and Deacon's lithostratigraphic members/submembers (after Deacon and Geleijnse [1988] and Wurz et al., [2022]). The depiction of the Cave 1B sequence, including the correlations between the two stratigraphic systems, reflects the results of this study. See Morrissey et al., 2022 for discussion of the presence or absence of MSA I–bearing deposits between the LBS and SAS in Cave 1A. (For interpretation of the references to color in this figure legend, the reader is referred to the web version of this article).

Figure 3. Lateral view of the KRM 41815/SAM-AP 6222 mandible (from the Deacon archive).

2022). It is therefore unsurprising that making stratigraphic correlations between both different parts of the site complex and different generations of excavation has proven to be a challenging task (Morrissey et al., 2022).

Very little information has been published on the stratigraphy of both the Wymer and Deacon excavations in Cave 1B, which complicates any assessment of the stratigraphic position of Layer 10 and KRM 41815 relative to Deacon's excavation units (Morrissey et al., 2022). In particular, Cave 1B lacks stratigraphic description and reconstruction of site formation processes, which hampers interpretations of human behavior that could be made from both the excavated assemblages and anthropogenic features and deposits.

Archaeological micromorphology and complementary microscale analyses have proven to be highly effective for identifying geogenic, biogenic, and anthropogenic depositional and post-depositional processes at MSA sites in the region (e.g., Goldberg, 2000; Miller et al., 2013, 2016; Karkanas et al., 2015; Haaland et al., 2021). As sedimentary stratigraphy is the product of site formation processes, microscale analyses can also provide important information for stratigraphic interpretation, especially in cases where the type or intensity of post-depositional processes have varied across a site or complex (e.g., Goldberg, 2000; Karkanas and Goldberg, 2010). Only relatively limited microscale research has been published on the KRM site complex to date, but these studies have provided important insights into site formation processes in Caves 1, 1A, and 2, including the human behaviors represented by anthropogenic features in these areas of the complex (Larbey et al., 2019; Wurz et al., 2022).

Here, we present the most detailed description of the stratigraphy of Cave 1B to date, and the first micromorphological data for this part of the site complex. These new data, along with previously published observations, are used to 1) better understand the formation of deposits in Cave 1B, 2) broadly correlate the deposits in Cave 1B with the rest of the KRM site complex, and 3) clarify the stratigraphic relationships between Layer 10 and Deacon's excavation units in order to confirm the cultural association of KRM 41815.

1.1. Past research on the Cave 1B deposits

Cave 1B is a relatively small, shallow shelter on the western side of the KRM site complex (Fig. 1). It is roughly 10 m wide at the outer edge of the excavated area, and the overhang covers only a few meters from the back wall outwards. The morphology of the hosting quartzite outcrop provides protection from coast-parallel easterlies and westerlies, but the shelter is very exposed to onshore winds from the south. As a result, the precipitation of salt onto various surfaces within the shelter due to sea spray is commonly observed. The formation of barrier dunes between the complex and the sea during parts of the Late Quaternary—as proposed by Deacon (1995)—could have provided greater protection from onshore winds than at present. The combination of these factors means that Cave 1B, while the most exposed area of the site complex, does enjoy some protection from rain, wind, and wind-blown sand. However, the degree of exposure would have varied over time, and across the extent of the shelter.

The deposits within the shelter have been truncated by erosion, most notably towards the seaward edge of the shelter, and there is increasing disturbance of deposits moving away from the shelter wall (Singer and Wymer, 1982). The current scree surface slopes steeply down from the southeast to the edge of the original excavation. Here, it is roughly 9 m above mean sea level (amsl). The lowest exposed bedrock within the shelter is at around 7 m amsl on the southern edge of Wymer's excavation (Henderson, 1992: fig. 3), just a little higher than the ~6-m quartzite wave-cut bench south of the site.

Cave 1B is physically separated from Cave 1 by the host rock (Fig. 1), and there are no recorded continuous deposits (either extant or excavated) between these two areas. It is possible that there were continuous deposits around the spur of rock joining them, perhaps related to activities taking place in the variably exposed cave, shelter, and open area between them based on the type of activity and changing weather conditions. However, this area is more susceptible to continuous processes of erosion and disturbance (like slope wash and trampling) and would have been more heavily impacted by coastal erosion during sea level high-stands. Therefore, the chances of any distinguishable interlinking deposits surviving to the present day are very low, particularly for anthropogenic deposits.

The Wymer excavations John Wymer excavated in Cave 1B in the years 1967–1968, digging several square meters of the shelter down to bedrock in a series of 15 layers (Fig. 1; Table 1). The sedimentary properties of the layers were described in very limited detail (Singer and Wymer 1982:24–25), and none were considered in Butzer's (1982) sedimentological study. No lithological correlations were made with the rest of the site except for the basal gravels (Layer 15), which were correlated with similar deposits in Cave 1 and 1A (Layer 40).

The layer descriptions followed guidelines for recording soil properties for engineering assessments, which do not distinguish between soils and sediments (Jennings and Brink 1961). As a result, the word ‘soil’ in the descriptions (Table 1) appears to largely be used synonymously with sediment, and, with the possible exception of Layer 13 and the disturbed deposits to the south of Wymer's excavation, there is no clear indication of any pedogenesis in Cave 1B from the published descriptions. Singer and Wymer's (1982) use of the term 'carbonaceous' denotes dark sediments rich in (mostly charred) organic matter, including both charcoal and finer material. It is unclear precisely how rich in this material the sediment had to be in order to be described in this manner. It is also unclear if the term ‘occupational soil’ was intended to be largely synonymous, or if this reflects a lower density of charred organic matter within the layer.

Singer and Wymer (1982) grouped their layers into cultural phases using the typological compositions of the lithic assemblages excavated from each layer. They assigned the entire Cave 1B sequence to the MSA I, correlating these deposits with the basal layers in Caves 1 and 1A. This was supported by the oxygen isotope values for marine shells from Layer 12, which were similar to those from Layer 38 in Cave 1 and suggested a Last Interglacial age (~120 ka) for the lower part of the Cave 1B sequence (Shackleton, 1982). The sequence was argued to represent fairly continuous occupation

Table 1
John Wymer's descriptions of the layers he excavated in Cave 1B (quoted from Singer and Wymer, 1982:24–25). The layers are numbered from the surface downward.[a]

Layer	Description
1	Sandy soil with some ash and small rock fragments. Artifacts were numerous, but only a small part of this layer remained, and they were mixed inadvertently with the underlying layer.
2	Buff [yellowish brown] sand, which contained small rock chips and rubble. The layer was silty in patches. Bones and artifacts were numerous.
3	This was a black carbonaceous soil with ash laminations and a spread of small, angular rock fragments at the base. Shells were decomposed to white flecks, but bone was in fair condition. Artifacts were numerous.
4	Same as the layer above without the rock fragments at the base.
5	Buff [yellowish brown] sand and small rock fragments, which thinned toward the shelter wall. The base was marked by a thin layer of carbonaceous soil. Artifacts were numerous, but only a few fragmentary bones and shells were present.
6	A gravelly to silty occupational soil with smears of ash hearths. Artifacts and bones were numerous, but the latter were in poor condition and were very fragmentary. Shells were scarce.
7	Buff [yellowish brown] sand and silty soil with many small, angular rock fragments. The numerous artifacts and many bones were in better condition than those in the layer above. Shells were scarce.
8	The surface of a thin (1–2 cm) but continuous hearth spread. There were several artifacts and bones, the latter in good condition. No shell was found.
9	Buff [yellowish brown] sand and silty soil with small, angular rock fragments. Several bone fragments were found in good condition, also shell fragments. Artifacts were numerous.
10	A dark gray clayey soil, which had many small, angular rock fragments at its base and one large block of soft calcite. It was flecked with charcoal but had no clear hearth spreads. Several bone fragments in good condition were recovered, including a near-complete human mandible (no. 41 815). Artifacts were numerous.
11	A firm buff [yellowish brown] sandy silt, which contained many small, angular rock fragments. A few bone fragments and several shells in good condition, as well as numerous artifacts, were found.
12	A thin, soft silty layer with a spread of loose, mainly burnt shell. Several bones in good condition and numerous artifacts were found.
13a	Brown sand that appeared to be a weathered horizon of the underlying layer. A few bone fragments, shells, and artifacts were recovered.
13b	Yellow sand and silt. Many bone fragments in a good, semimineralized condition, a few shells in poor condition, and numerous artifacts were found.
14	A thin (2–4 cm) spread of carbonaceous soil with small fragments of shell. On the south side lay two large fallen blocks of the rock wall or overhang: one is featured in the drawn section. Several bones were found in good mineralized condition. Artifacts were numerous.
15	Clean, angular, sandy beach gravel. Artifacts were numerous in the upper part, and there were a few bone fragments but no shells.

[a] All square parentheses and content therein are added by the authors.

of the shelter during the MSA I, following regression from the peak of the Last Interglacial sea-level highstand, with the weathering of Layer 13 viewed as representing the only evidence for a depositional hiatus during this period (Singer and Wymer, 1982:25).

Lewis Binford (1984) challenged some of the interpretations made by the original excavators and their collaborators. He argued that the species composition of the faunal assemblages published by Klein (1976) from Cave 1B suggested that these layers were contemporaneous with the HP or MSA III layers in Cave 1A or had an age falling between these deposits. Singer and Wymer (1986) defended their original position, pointing to differences in lithic typology between the HP and MSA III and the assemblages from Cave 1B, and stressing that the Cave 1B deposits and the MSA I layers in Caves 1 and 1A formed on similar gravels at the base of these respective recesses. Binford (1986a) responded by highlighting some apparent similarities in typological and raw material characteristics between the Cave 1B assemblages and the HP and MSA III and by arguing that deposits of varying ages could have formed on the same beach gravels. The faunal data were subjected to two distinct sets of multivariate analyses. Neither found a correlation between Cave 1B and the MSA I fauna from the rest of the site, instead suggesting greater similarity with the MSA II for one study (Thackeray, 1986) and the HP, MSA III, and MSA IV for the other (Binford, 1986b).

The Deacon excavations Deacon dug a 1-m^2 sampling square (PP38) into the western profile of the Wymer excavation but did not reach bedrock (Fig. 1). A larger surface excavation was carried out to the west of PP38, which sampled some of the upper units over an area of 3 m^2 (Henderson, 1990, 1992). Both excavations were conducted at significantly higher stratigraphic resolution than Wymer's, with distinct deposits excavated as individual excavation units so far as practical.

Based on broad lithological similarities between the Cave 1B deposits and those in Cave 1 and 1A, the sequence was split into two members, interpreted as being equivalent to the LBS and SAS Members in Caves 1 and 1A (Deacon and Geleijnse 1988:11). Only the basal deposits above the gravel were assigned to the LBS, with the bulk of the sequence placed in the SAS Member (Deacon and Geleijnse, 1988: figs. 5 and 6). The SAS was later revealed to have been split into two submembers, the Rubble Sand (RS) and Dark Carbonized (DC; Henderson, 1992: fig. 3). It was argued that Wymer's Layer 13 (and hypothesized hiatus) could correlate with a similar event proposed for unit YS1 in AA43/Z44 at the Cave1/1A boundary (Deacon and Geleijnse, 1988). However, deposits overlying Layer 13 were also correlated with deposits underlying YS1 (Deacon and Geleijnse, 1988:11), suggesting that these proposed hiatuses represent different events (see Morrissey et al., 2022:21).

As with Butzer's work during the initial excavations, no sedimentological data were published for Cave 1B by Deacon and Geleijnse (1988). An unpublished report (Deacon et al., 1986) includes the grain-size properties of two bulk sediment samples from Cave 1B, but it is unclear if further samples were analyzed, and why the results presented in the report were never published. The unit names given with the samples do not match any of the excavated units in PP38 or the larger surface excavation, preventing the use of the data to characterize any of these deposits.

The area of excavation adjacent to PP38 sampled the uppermost portion of the DC, revealing a sequence of alternating sandy units and more stratigraphically complex groups of units containing deposits interpreted as being largely anthropogenic in origin (Henderson 1992). As with similar deposits across the site complex (e.g., Deacon, 1993, 1995), the latter units were called carbonized partings (CPs), except for one which was designated as a partly carbonized parting (PCP), the only published occurrence of the use of this term at Klasies.

It was noted that the stratigraphy was poorly preserved near the shelter wall, grading into a homogenous gravelly sediment perhaps due to disturbance by water movement (Henderson, 1990:37). Little information was provided on the sandy units as the anthropogenic deposits were the focus of the study. The anthropogenic units include concentrations of ash, shell, bone, and carbonized (or partly carbonized) organic matter (Henderson, 1992). Concentrations of shells were interpreted as "small shell disposal features" (Henderson, 1992:25), representing discard of food waste in specific locations but on a smaller scale than the middens preserved in other parts of the complex. The clustering of ash features, especially prevalent in the lowermost excavated anthropogenic unit, was interpreted as the result of repeated fires being made in a single part of the shelter. These features are argued to represent organization of space within the shelter by the people occupying the shelter during this period.

Other than these interpretations, almost no information on site-formation processes in Cave 1B is available (Morrissey et al., 2022: tables 3 and 4). Furthermore, none of the units in the area excavation were correlated to any of Wymer's layers (Henderson, 1992).

A single relative date for Cave 1B was obtained by Goede and Hitchman (1987). Their electron spin resonance dating of marine shell fragments suggested a temporal correlation between Layer 10 (and KRM 41815) and Layer 37 in Cave 1. However, this result must be treated with caution as it appeared that rates of uranium enrichment varied across KRM and through the sequence (Goede and Hitchman, 1987:171–172).

A techno–typological analysis of lithic artifact samples from Deacon's excavations across KRM concluded that the Cave 1B sequence included a lower MSA I phase and an overlying MSA II phase (Thackeray, 1989:52). This pattern was confirmed through further detailed techno–typological research by Sarah Wurz (2002), who recognized two cultural subgroupings within the MSA II, the MSA II lower, and MSA II upper (or Mossel Bay lower and upper). Wurz (2002) was the first to publish correlations between the excavation units in PP38 and Wymer's layers (see also note in Grine et al., 2017b:57). These correlations were made based on Deacon's interpretations of unpublished data and only correlated cultural groupings (and their associated excavation units) with groups of Wymer's layers, rather than correlating specific units with layers (Table 2).

The placement of Layer 10 within the MSA II corresponds with Deacon's repeated assessment that KRM 41815 is roughly contemporaneous with a hypothesized event involving the cannibalization and discard of the remains of multiple individuals in Cave 1 early in the MSA II cultural phase (Deacon and Schuurman, 1992; Deacon, 1995, 1998, 2008). The apparent contradiction between Layer 10 being correlated with MSA II deposits while sharing a similar relative date with the MSA I–bearing Layer 37 was never addressed. The association of a significant portion of the PP38 sequence with the MSA I (Wurz 2002) was also never dealt with, despite Singer and Wymer's (1982) figure 3.14 showing that the specimen was recovered relatively low down within their excavation. Grine et al. (2017b:57) subsequently suggested that the PP38 units Deacon correlated with Layers 10 and 11 should be correlated temporally with the 'RBS' Member/Layer 37 (thus attributing the mandible to the MSA I) but did not provide any supporting evidence or discussion. This paper will provide more stratigraphic resolution and allow the development of a firm hypothesis for the age of the mandible.

Table 2
Summary of the published stratigraphy of both phases of excavation in Cave 1B (data from Singer and Wymer, 1982; Deacon and Geleijnse, 1988; Henderson, 1992; Wurz, 2002).

Wymer excavations		Deacon excavations		
Excavation units	Cultural stratigraphy	Excavation units	Lithostratigraphic members/submembers	Cultural stratigraphy
Layer 1	MSA I	DC surface to DCCP6	Dark Carbonized/Shell and Sand	MSA II upper
Layer 2				
Layer 3				
Layer 4				
Layer 5				
Layer 6		DCCP7 to DCCP12		MSA II lower
Layer 7				
Layer 8				
Layer 9				
Layer 10				
Layer 11				
Layer 12		RSYS1 to RSBCH	Rubble Sand/Light Brown Sand	MSA I
Layer 13a and b				
Layer 14				
Layer 15				

Abbreviations: DC, Dark Carbonized; MSA, Middle Stone Age.

2. Materials and methods

2.1. Field description of stratigraphic units

The excavation units defined by the Deacon team were identified in the three profiles (northern, western, and southern) of square PP38 based on their stratigraphic drawings and labels they had placed on the profiles (Figs. 4–6). The units were then described based on macroscopic observation in the field in 2020. Variables recorded include the texture and color of the matrix, the nature of any clasts (including artifacts) within the unit, whether contacts between units are sharp or diffuse, and the presence of finer stratification within a unit. Due to the fine and complex stratification of many of the deposits referred to as CPs, the Deacon team grouped some excavation units into a single CP in multiple cases. For consistency, these groupings were used in the field descriptions.

2.2. Microanalysis of thin sections

Three micromorphology blocks (KRM-13-10, KRM-13-11, and KRM-13-12) were collected in 2013 in a column near the eastern edge of the northern profile of PP38 in 2013 (Figs. 4 and 6). The column includes the upper portion of the MSA I–bearing RS and most of the MSA II lower deposits in the DC. The blocks were carved and plastered with gypsum bandage to allow the removal and transport of intact sediments.

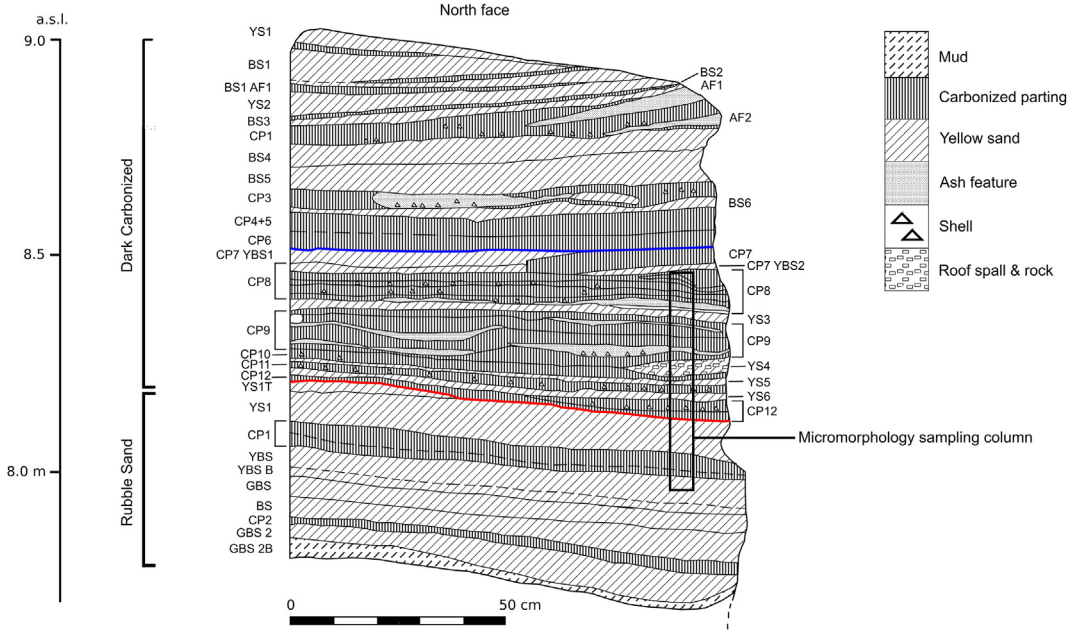

Figure 4. A partial stratigraphic drawing showing the excavation units for the northern profile of square PP38 (profile redrawn by L. van Pletzen Vos from the original field drawings by the Deacon team). The rest of the profile is shown in Figure 6. The red line indicates the boundary between the Middle Stone Age (MSA) I and MSA II lower, and the blue line shows the transition from the MSA II lower to the MSA II upper (following Wurz, 2002). Due to the complex and finely stratified nature of the deposits in the Dark Carbonized, the individual excavation units Deacon grouped into the Carbonized Partings are not labelled. (For interpretation of the references to color in this figure legend, the reader is referred to the web version of this article).

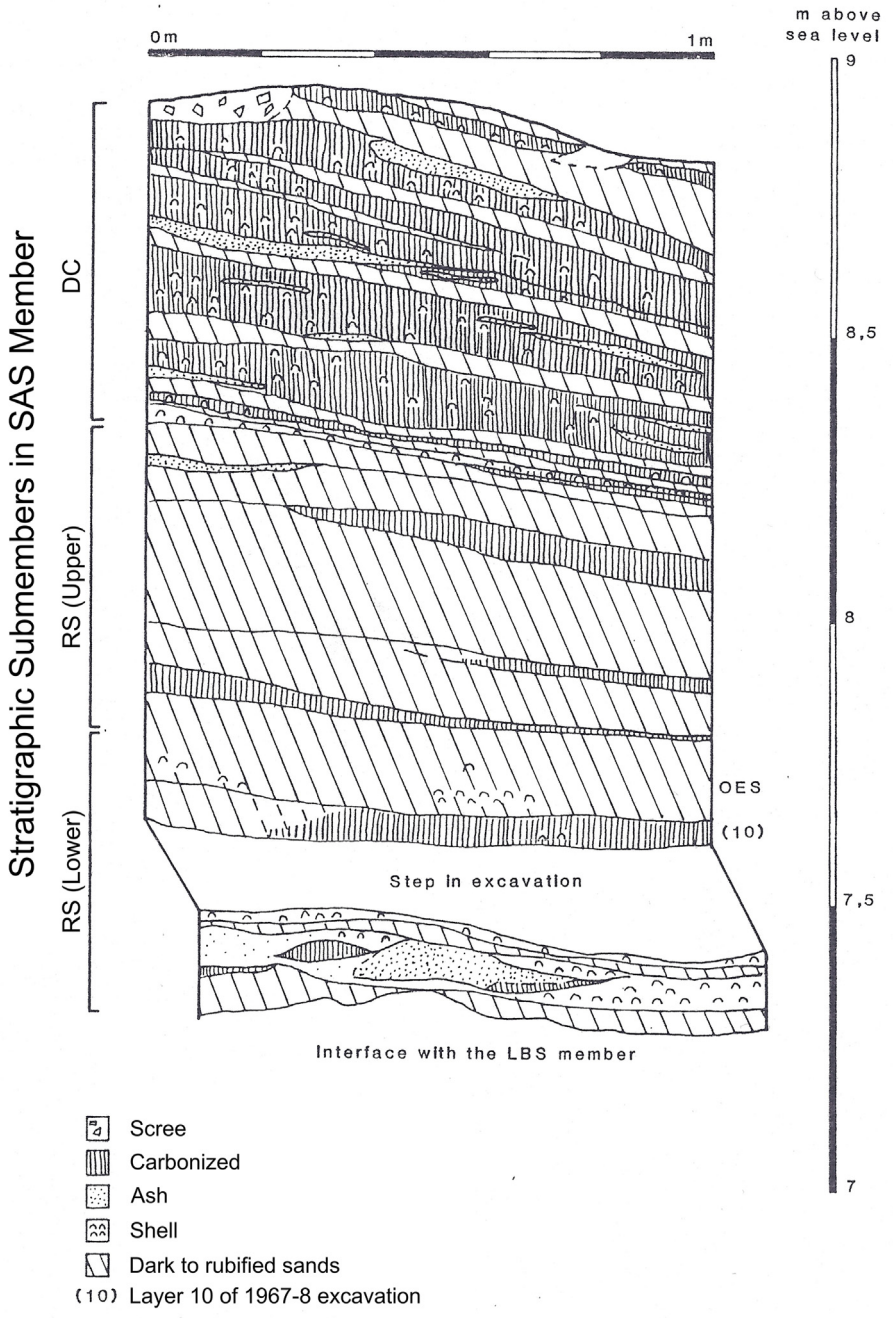

Figure 5. A previously unpublished drawing of the western profile of PP38 (Deacon archive), including the step and the contact with the unexcavated LBS. In contrast to Figure 4, this drawing shows the full extent of the excavation, but shows less stratigraphic detail and lacks unit labels. Note the suggested correlation for Layer 10 directly above the step.

Block KRM-13-12 includes the top of unit RSYBS, the vertical extent of RSCP1 and RSCP1T, and the base of RSYS1. KRM-13-11 samples the upper portion of RSYS1, the vertical extent of DCCP12, DCYS6, and DCCP11. KRM-13-10 includes part of DCYS4 at its base, along with the vertical extent of DCCP9 and DCYS3, and the majority of DCCP8.

After transport to University of Tübingen, the blocks were dried, indurated with a mix of resin and styrene and then were processed into seven thin sections. Micromorphological analysis of the thin sections was carried out using a petrographic microscope at a variety of magnifications under both plane-polarized and cross-polarized light. Description of the sediments followed standard terminology (Stoops, 2021). The sections were also analyzed using a Bruker M4 Tornado micro-X-ray-fluorescence (μXRF) analyzer to produce elemental maps of each section to supplement the micromorphology (Mentzer, 2017). As detailed in Wurz et al. (2022) for the analysis of thin sections from the rest of the KRM complex, the following parameters were used: dual detectors, 60-micron pixel spacing, ~25-micron spot size, 50-kV rhodium tube voltage, and a 600-microamp current. The micromorphology observations and the distribution of key elements in the elemental maps were used together to identify and describe microstratigraphic units (MSUs). Elemental overlay maps for each thin section are provided in the figures of this paper to help the readers see important

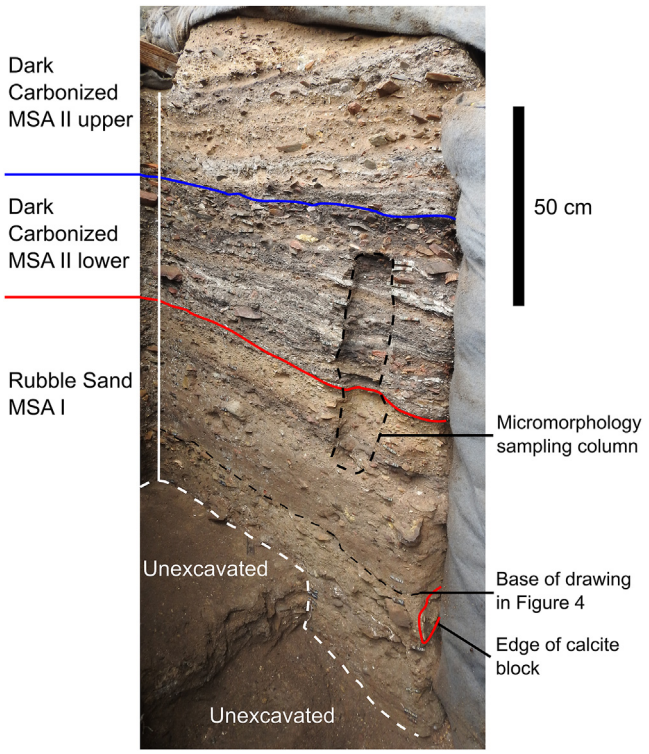

Figure 6. Photograph of the northern profile of square PP38, which includes the deposits not shown in Figure 4. As the photograph was taken in 2020, the sampling column from 2013 has been eroded slightly. Note the step in the excavation and that bedrock has not been reached anywhere in the square. The calcite block (Fig. 8) visible in the western profile of the original excavation is present in Singer and Wymer's (1982) figure 3.14 and plate 26 (see further discussion in text), and in photographs taken during the Deacon excavations (see Fig. 7). (For interpretation of the references to color in this figure legend, the reader is referred to the web version of this article).

sedimentary components such as shell and bone. The microfacies approach (Courty, 2001) was used to classify the numerous MSUs identified in the samples into categories of deposit with similar formation histories.

3. Results

3.1. The macrostratigraphy of square PP38

Deacon's excavation in PP38 did not reach bedrock, and the basal beach gravel described by Singer and Wymer (1982) is not exposed. The unexcavated deposits were assigned to the LBS Member by Deacon (Fig. 5). The exposed profiles include roughly 1.8 m of deposits. The only detailed profile drawings with labelled excavation units (e.g., Fig. 4) were drawn prior to the completion of the excavation, excluding multiple excavation units and up to 30 cm of deposit (at the deepest point) from the drawings (Figs. 5 and 6). There is a step at the base of the excavation, with only a ~20-cm-wide strip excavated along the eastern edge of the square (Figs. 5 and 6). The units excavated there are thus only exposed in the northern and southern profiles. They are the only units in PP38 not included in Wurz's (2002) lithic analysis, perhaps due to limited sample sizes. As they underlie units assigned to the MSA I, it is reasonable to assume an association with this technocomplex.

Descriptions of the PP38 excavation units are presented in Table 3. Throughout the text, the unit abbreviations include RS or DC as prefixes to indicate which group of deposits each unit falls within. Full unit names are provided with the descriptions in Table 3. Due to the finely stratified nature of many deposits in the DC, a single description is provided for each of the CP unit groups.

The exposed deposits throughout the sequence generally dip down towards the back of the shelter (north) when viewed in the western profile. Dip angles along the east–west axis (observed in the northern and southern profiles) are shallower and more variable in direction, but the majority dip down towards the east. The deposits are often thicker in the southern profile than in the northern, especially in the RS.

The RS is dominated by deposits of varying shades of light brown, gray, and yellowish silty sand. Clay is present, but there is a notable reduction from RSBS upward. Likewise, there is a significant increase in the density of quartzite fragments from RSYBSB (a few units above RSBS) upward, and microfauna remains are first visible from the same point in the sequence. Materials introduced by anthropogenic processes—including lithic artifacts, charcoal, bone fragments, shell, and (what appears to be) rubified quartzite—are present in almost all units. Deposits seemingly formed through significant anthropogenic inputs are limited to occasional lenses rich in carbonized material in the sand units and in units RSCP2, RSCP1, and RSCP1T. The contacts between units are typically relatively diffuse throughout the RS, with many units grading into the overlying unit. The DC is initially dominated by ash lenses, shell-rich layers, and dark charred organic-rich deposits grouped into CP unit groups, which are interbedded with relatively thin sandy units. Most of the CPs also contain thin laminae or lenses of sand. From DCBS5 upwards, the sandy units become thicker, and the CPs thin notably (Fig. 4). The deposits in the CPs are often very finely bedded but typically thicken towards the south of PP38. Lateral changes in sedimentary properties across the extent of a CP are common, with shell density increasing markedly to the south in most units which contain shell. The sandy units are a variety of shades of brown, gray, and yellow. Most contain at least some material of anthropogenic origin, and thin black lenses are present in some of these units. Quartzite fragments are common in the sandy units except for DCYS6. The density of these clasts increases from DCBS6 upwards, and microfauna remains are observed from the same point in the sequence. Contacts between deposits are typically sharper than in the RS, especially within CPs and between CPs and sandy units. However, some relatively diffuse contacts were observed, especially between sandy units.

Correlating the PP38 excavation units (Table 3) with Wymer's layers (Table 1) is not straightforward due to the difference in stratigraphic resolution and the observed spatial variation in unit sedimentary properties. However, a relatively large piece of calcite recorded in Wymer's excavation profile (Singer and Wymer 1982: fig 3.14 and plate 26) is still present just to the north of PP38. It is only partially visible behind the protective sandbag wall erected by the Deacon team along Wymer's profile on either side of PP38 (Fig. 6), but drawings (Henderson 1992: fig. 3) and previously unpublished photographs from the PP38 excavation (Figs. 7 and 8) show it is the same as the one recorded by Wymer. This provides a vital anchor point for correlating between the two stratigraphic systems.

The calcite block is shown to lie mainly within Layer 9 of the original excavation (Singer and Wymer, 1982: fig. 3.14) but is listed as being in Layer 10 in the layer descriptions (Table 1). This suggests that the base of the rock is within Layer 10. The top of the block corresponds roughly with the base of unit RSGBS2B in PP38, and its lowermost point is near the top of unit RSBCH. The recorded properties of RSBCH (Table 3) are broadly consistent with the description of Layer 10 (Table 1), further supporting this correlation. KRM 41815 was assigned to Layer 10, its stratigraphic position was indicated as being just level with the base of calcite block, and it was found next to the block (Singer and Wymer, 1982:146).

Table 3
Basic descriptions of the excavation units visible in the profiles of square PP38 in Cave 1B. A single description is provided for each of the carbonized parting unit groups in the Dark Carbonized deposits due to the fineness and complexity of the stratification of most of these deposits. The full name of each unit (as inferred from the abbreviated names by the authors) is given in parentheses after its description.

Unit	Description
Rubble Sand	
BR	Not excavated completely—up to 5 cm in maximum excavated thickness. Slightly reddish light brown silty fine sand with some grit and clay. Clasts are rare and include shell and small lithics. (Brownish red)
BSH2	~Four- to 5-cm-thick light brown silty fine sand with grit and clay. Clasts slightly more common than in BR and include rare bone and lithics. Some dispersed charcoal flecks. (Brown shelly 2)[a]
BYS1	Up to 6-cm-thick yellowish light brown silty fine/medium sand with some grit. Clasts more common and include quartzite fragments, very small pebbles, shell, and bone. Some quartzite appears to be rubified. Shell preservation variable. (Brownish yellow sand)
BSH1	Not distinguishable in profile between BYS1 and BCH. (Brown shelly 1)
BCH	First unit above the small, stepped excavation. Up to 10-cm-thick light brown silty fine sand with some clay. Clast density higher than units in stepped excavation. Lithics, bone, small pebbles, and well-preserved shell all observed. Charcoal flecks common and regularly distributed. Some very thin dark lenses with limited lateral extent visible. (Brown charred)
Y/SH	Up to 8-cm-thick yellowish light brown silty fine sand with some clay. Clasts relatively rare, but often concentrated in patches. Variably preserved shell found both dispersed through the sand and in short 'lines' of several shells. Lithics and quartzite fragments also observed. Small charcoal fragments dispersed throughout. (Yellow shelly)
DRU	Up to 6-cm-thick light brown silty fine sand with clay and grit. High density of quartzite fragments, but variable across the unit, with some areas almost clast-free. Most pieces are under 5 cm in length, but many are larger—up to 14 cm. Fragments show preferred dip towards the east and south, matching the general dip of the deposits. Grit often found in concentrated pockets between larger clasts. Shell, bone, and lithics are all rare. (Dark rubble unit)
YRU	Up to 4 cm thick. Almost identical to DRU except that the matrix is yellower in color. Includes a single thin dark lens in the southern profile. (Yellow rubble unit)
GBS2B	Lowermost unit included in the Deacon profile drawing of the nothern profile. ~2.5- to 5-cm-thick slightly grayish brown silt with clay. Clasts are very rare and widely dispersed and are almost exclusively quartzite fragments (some of which appear to be rubified). (Grayish brown sand 2 base)
GBS2	~Three- to 10.5-cm-thick slightly grayish brown silty fine sand with some clay. Clast properties the same as in GBS2B. (Grayish brown sand 2)
CP2	~Two- to 3-cm-thick dark grayish brown silty fine sand with charcoal flecks and relatively large pieces. Only present in the northern and western profiles. (Carbonized parting 2)
BS	~Four- to 10-cm-thick light brown silty very fine sand. Clasts relatively uncommon and widely dispersed. Mainly quartzite fragments, but some shell in varying condition in southern and western profiles. (Brown sand)
GBS	~Four- to 10.5-cm-thick grayish light brown silty fine sand. Clasts similar to BS. (Grayish brown sand)
YBSB and YBS	~4.5- to 13-cm-thick yellowish light brown silty fine/medium sand with some grit. Relatively high clast density, with some concentrated patches. The clasts include bone, lithics, and quartzite fragments. Some of the bones are recognizable as microfauna. Rare charcoal flecks dispersed through the units. (Yellowish brown sand base and Yellowish brown sand)
CP1	~One- to 6-cm-thick dark silty sediment with some sand and grit that is rich in carbonized material. Some charcoal pieces visible. Clasts are relatively rare and include decayed shell and small quartzite fragments (with many apparently rubified). In the western profile, a lens of yellowish-brown gritty sand is present across much of CP1, splitting it almost in two. In the southern profile, the unit is limited to the eastern edge of the profile. Here, the dark sediment contains little visible sand and, unlike in the other profiles, there are distinct ash lenses or pockets overlying the dark sediment. (Carbonized parting 1)
CP1T	~Three- to 4.5-cm-thick very dark brown silty fine sand with significant grit and many charcoal flecks. Thin black lenses are common. Clasts include lithics, quartzite (with some apparently rubified), and very rare shell. This unit is only present in the northern profile. (Carbonized parting 1 top)
YS1	~Five- to 14.5-cm-thick yellowish silty fine/medium sand with a significant grit component. Small quartzite fragments (mostly between 3 and 5 cm in length) are extremely common throughout. Microfauna bones visible across the unit. Other clasts are fairly limited and include larger quartzite fragments, lithics, shell fragments, bone fragments, and charcoal (exclusively in the western profile). Several lenses of black sediment and/or ash are present in YS1 or between YS1 and YS1T in the western and southern profiles. (Yellow sand 1)
YS1T	~0.5- to 1.6-cm-thick unit very similar to the underlying YS1. The major differences are that the matrix in YS1T is somewhat darker in color and slightly finer in texture, and that lithics, bone, shell, and charcoal are all notably more common. Uppermost unit associated with the MSA I. (Yellow sand 1 top)
Dark Carbonized	
CP12	~0.5- to 4.5-cm-thick spatially variable package of deposits with both vertical and lateral contacts between distinct deposits. Deposits include sediment rich in charred organic material, brown sand, and gray sand with dark patches, dispersed shell, and ashy laminae. The shell is typically fairly degraded and often forms layers which can be tracked within the matrix even when the shell is relatively dispersed. Charcoal is common throughout the deposits. Other clasts very rare. Lowermost units associated with the MSA II lower. (Carbonized parting 12)
YS6	Up to 3-cm-thick grayish light brown silty medium sand with some faint darker lenses. Clasts are rare and mostly quartzite fragments <1cm in length. Absent in the southern profile and somewhat discontinuous in the northern and western profiles. (Yellow sand 6)
CP11	Up to 1.5-cm maximum thickness. On the eastern end of the northern profile, it comprises black sediment rich in charred material with no shell. Across much of the northern and western profile, it is a very thin lamination of broken shell with some black sediment and charcoal. However, there are also patches of more concentrated shell. Indistinguishable from CP12 in southern profile due to the absence of YS6 in this profile. (Carbonized parting 11)
YS5	Up to 5-cm-thick brown silty medium sand. Quartzite fragments are common, while lithics, bone, and shell are less so. Shell and charcoal are typically dispersed, but there are some concentrations of shell. Often difficult to identify in the northern profile (and less commonly in the western profile) between CP11 and CP10. (Yellow sand 5)
CP10	~One- to 4-cm-thick unit comprising dark sediment rich in charred organics and several distinct ash lenses. Small quartzite clasts common, including some which appear to be rubified. Shell present but rare. (Carbonized parting 10)
YS4	Wedge-shaped deposit present on the eastern edge of the northern profile and across the eastern half of the southern profile. Up to 6-cm-thick on profile edges. Dark gray silty fine sand matrix with significant grit component. Clast density very high, mostly quartzite fragments under 4 cm in length, many of which appear rubified. Some lithics present, along with very rare bone fragments and dispersed charcoal. (Yellow sand 4)
CP9	~Nine- to 12-cm-thick package of alternating laminated to bedded deposits of black charred organic-rich sediment, ash, gray sand, and shell. Clast density is fairly high, with quartzite fragments, small pebbles, lithics, and very rare bone all present. Some quartzite appears rubified. Shell is relatively rare and dispersed in places, but there are also distinct layers of dense compressed shell. Charcoal visible throughout. Typically, more finely laminated in the northern profile than in the western and southern ones. Relatively difficult to distinguish from the underlying CP10 except where YS4 is present. (Carbonized parting 9)
YS3	~1.5- to 3-cm-thick brown medium sand with some grit. Quartzite fragments common, particularly smaller pieces (<1 cm). Lithics present by not common. Shell and charcoal dispersed throughout, but the density of shell increases notably in the southern profile. (Yellow sand 3)
CP8	Up to 15-cm-thick package of deposits including laminated to finely bedded ash, black carbon-rich sediment, and gray sand with dispersed carbon. Paler sand lenses are also present but have limited lateral extent. Quartzite fragments (some seemingly rubified), lithics and bone present throughout. Shell is mostly poorly preserved. The deposits are notably more coarsely bedded, less clearly defined, and richer in shell moving towards the southern profile.

Table 3 (*continued*)

Unit	Description
	Capped by a deposit of brown sand with relatively faint black lenses. Dispersed shell and charcoal flecks present throughout, along with some lithics and bone. Lithic artifacts and quartzite fragments occur at a higher density than the rest of CP8. (Carbonized parting 8)
CP7	Up to 5.5-cm-thick package of relatively thickly bedded deposits including black sediment rich in charred material, dark gray sand, and ash packets of varying lateral extent and thickness (up to 6 cm thick). Charcoal is common but varies in density. Shell is rare and mostly absent from northern profile. Clasts relatively common and include quartzite fragments and lithics. The base of CP7 is a deposit of dark silty sand, which is extremely clast-rich on the western edge of the square but has a far lower clast density across the rest of the square. Uppermost units associated with the MSA II lower. (Carbonized parting 7)
CP6 to CP4	Up to 13-cm-thick package of laminated to relatively thickly bedded deposits. Deposits include ash, black charred organic-rich sediment, yellowish light brown sand, brown sand, and dark gray sand. Bedding thickness increases for most deposits moving towards the south. Shell is virtually absent in the northern profile but is found in multiple distinct laminae across the western and southern profiles. Charcoal flecks common throughout. Quartzite fragments and lithics present at low density throughout. Lowermost units associated with the MSA II upper. (Carbonized partings 6 to 4)
BS6	~0.5- to 3-cm-thick yellowish light brown sand with very rare charcoal and dispersed shell. Quartzite fragments common, as are microfauna remains. Some bone fragments and lithics observed. Matrix grayer in the western profile. Not present in southern profile. (Brown sand 6)
CP3	Up to 9-cm-thick package of deposits ranging in thickness from laminae to relatively thick beds. Deposits include yellowish light brown sand, black sediment rich in charred material, and shell-rich layers. Thicker deposits often include lenses of other material. Shell density increases notably moving towards the south. Quartzite fragments, bone, and charcoal are all reasonably common, but dispersed through the deposits. Largely indistinguishable from CP4 in the southern profile due to the absence of BS6. (Carbonized parting 3)
BS5	~2- to 7.5-cm-thick light brown medium sand with some rare faint darker laminae. Most clasts are small (<0.5 cm) quartzite fragments, but larger quartzite pieces and lithics are also common. Shell is present but very rare and some microfauna remains observed. Charcoal flecks common, but largely found in a few concentrated patches. Not preserved in southern profile. (Brown sand 5)
BS4	~2.5- to 6.5-cm-thick alternating laminae of light brown sand, yellowish brown sand, and black lenses. Quartzite fragments are typically small, but there are a few concentrations of larger pieces. Lithics, bone and some charcoal observed throughout, along with microfauna remains. Not preserved in southern profile. (Brown sand 4)
CP1	Up to 8-cm-thick package of laminated to thinly bedded deposits of ash, shell, gray sand, and black carbon-rich sediment. Charcoal and lithics are common throughout. Most clearly stratified on the western edge of the northern profile. Moving across and into the western profile, the package is dominated by beds and laminae of black sediment and shell. Moving across the western profile, the shell density gradually increases, but black laminae remain. Not preserved in southern profile. (Carbonized parting 1)
BS3	Up to 2.5-cm-thick light brown sand. Clasts are relatively rare and include isolated quartzite fragments and a single piece of bone. Charcoal flecks throughout. Only preserved in the northern profile. (Brown sand 3)
BS2	~0.5- to 2-cm-thick brown medium sand. Clasts relatively common and include lithics, quartzite fragments and rare shell. Charcoal flecks throughout and more common than in BS3. Only preserved in the northern profile. (Brown sand 2)
YS2	~2.5- to 5-cm-thick yellowish brown medium sand. Quartzite fragments are common, as are microfauna remains. Only preserved in the northern profile. (Yellow sand 2)
BS1	Up to 8-cm-thick light brown to brown fine/medium sand, with a ~1-cm-thick layer of black sediment and ash at its base. Clasts are common and include lithics, microfauna remains and quartzite fragments (some of which appear rubified). Charcoal flecks throughout. Only preserved in the northern profile. (Brown sand 1)
YS1	Heavily eroded yellowish light brown sand with quartzite fragments. Original thickness unclear. Only preserved in the northern profile. (Yellow sand 1)

[a] No shell was observed in RSBSH2, but this unit has a very limited exposure in the profiles of the stepped portion of the excavation. It is likely that this deposit was richer in shell towards the center of the excavation (and perhaps further east into Wymer's excavation) but contained little shell on its edges.

Therefore, it must relate to RSBCH. This matches the suggested correlation in the previously unpublished Figure 5. This correlation places the specimen unambiguously within the MSA I deposits.

Based on the descriptions of the layers and units and visual comparison of the Wymer and PP38 profiles, correlations can be made or suggested for much of the sequence (Table 4). A few of the more significant correlations, and those with either less clear boundaries or less secure correlations, are presented in more detail here:

1. RSCP2 is the only unit with properties similar to Layer 8 that falls within roughly the right part of the sequence. However, as it is somewhat higher up the profile than Layer 8 is depicted in the original profile drawing, there is an element of doubt in this correlation.
2. The uppermost MSA I deposits—units RSYS1 and RSYS1T—correspond well with both the description and depth of Wymer's Layer 5. However, it is possible that the underlying RSCP1T could have been the base of Layer 5, rather than part of Layer 6.
3. The DC below the marked increase in thickness of sandy units (from the base of DCBS5) is correlated with Layers 4 and 3. The gravel-rich base of Layer 3 corresponds best with the gravel unit at the base of DCCP7. DCYS4 also matches the description of Layer 3's base, but this would make Layer 4 thinner than it is depicted by Wymer. With either boundary, the transition from the MSA II lower to the MSA II upper (the contact between DCCP7 and DCCP6) falls within Layer 3.
4. Due to erosion and the slope of the shelter surface, it is not entirely clear where the top of Wymer's profile would have been relative to the sloping tops of PP38's northern and southern profiles.

It can be assumed that the unexcavated deposits in PP38 must broadly correlate with the rest of Wymer's sequence. As these deposits cannot be observed without removing the supporting sandbag walls along Wymer's profile—which could result in significant collapse and loss of deposit, even with carefully planned mitigation—there are no data with which to confirm this assumption.

3.2. Microstratigraphy

More than 70 MSUs were identified within the seven micromorphology slides analyzed (Figs. 9–11). These MSUs are assigned to one of 12 microfacies (MF) types, which are described in Table 5. Representative photomicrographs for each of the MFs are provided in Figs. 12–14. The microstratigraphy of the samples is detailed below, following the excavation units (or unit groups where more appropriate) utilized by the Deacon team.

Unit RSYBS (Fig. 9) is the lowest excavation unit represented in the thin sections and falls within the MSA I–bearing RS. The sampled portion comprises three MSUs of ashy sand with quartzite clasts, bone, shell, and charcoal (MF 1.2.1). The size and density of the coarse inclusions and the amount of ash in the matrix all vary between the MSUs. The quartzite and bone fragments are

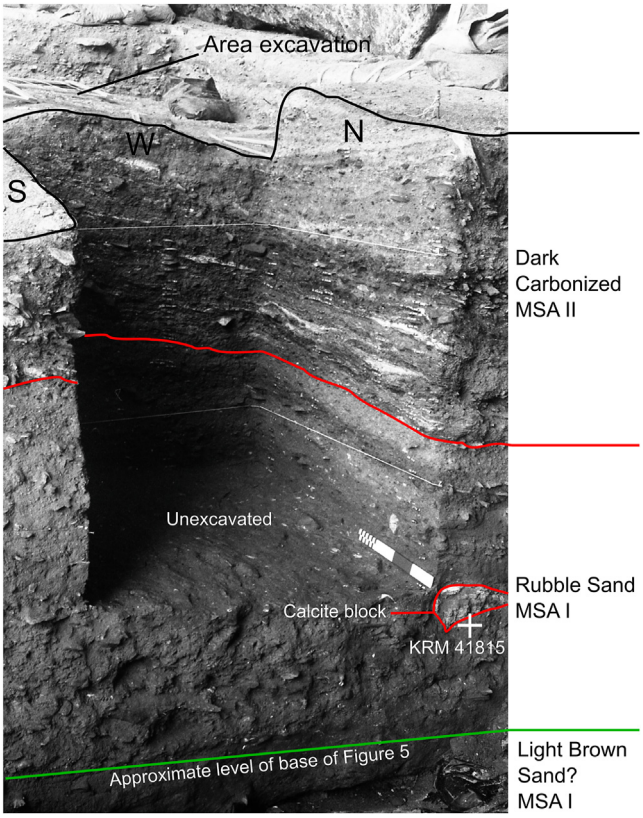

Figure 7. Photograph of square PP38 taken during the Deacon excavations from the eastern side of Cave 1B (from the Deacon archive). The scale bar is 40-cm long, and the base of the excavated portion corresponds roughly with the drawing in Figure 4. Note the calcite block which is depicted in a site photograph and profile drawings from the original excavation and still visible in the section (Figs. 6 and 8). The white cross shows the approximate stratigraphic position of KRM 41815 as depicted in Singer and Wymer's (1982) figure 3.14. (For interpretation of the references to color in this figure legend, the reader is referred to the web version of this article).

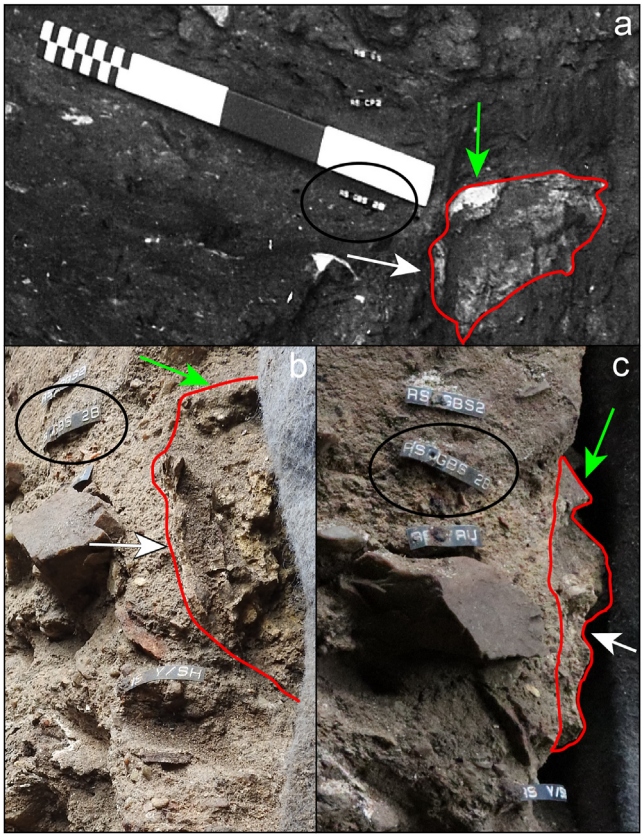

Figure 8. Multiple views of the calcite block (outlined in red) in Wymer's western profile, adjacent to PP38. a) View from the southeast during the excavation of PP38 (scalebar is 40 cm), b) View from the east in 2020, and c) View from the south in 2020. The arrows indicate parts of the block visible in all three views. The green arrow (upper) and white arrow (lower) each point to the same part of the block in each view. Note Deacon's label for unit RSGBS2B (circled in black). (For interpretation of the references to color in this figure legend, the reader is referred to the web version of this article).

significantly larger in the lowermost MSU. The arrangement of several relatively large clasts in a rough line at the base of the third MSU is suggestive of a possible surface. Some small coprolites were observed towards the base of the unit.

Unit RSCP1 (Fig. 9) is composed mainly of ash with some sand, small quartzite fragments, shell, and charcoal (MF 3.2). Finer charred organic material is present throughout but is most highly concentrated in a thin deposit, which also contains numerous very small charcoal pieces (MF 4.1). There is also a small zone of significantly sandier and less ashy sediment, with a relatively high density of small quartzite fragments (MF 1.2.1).

Table 4
Revised correlations between the different stratigraphic systems utilized in Cave 1B, moving down from the surface. Layers 13b, 14, and 15 are believed to fall within the unexcavated portion of the sequence in what Deacon and Geleijnse (1988) considered to be the LBS Member.

Layer	PP38 excavation unit or unit group	Lithostratigraphic members/submembers	Cultural stratigraphy
1	DCCP1 upward[a]	Dark Carbonized	MSA II upper
2	DCBS5 and DCBS4		
3	DCCP7 to DCCP3[a]		MSA II lower
4	DCCP12 to DCCP8[a]		
5	RSYS1 and RSYS1T[a]	Rubble Sand	MSA I
6	RSCP1 and RSCP1T[a]		
7	RSBS to RSYBS		
8	RSCP2[b]		
9	RSY/SH to RSGBS2		
10	RSBCH		
11	RSBYS1		
12	RSBSH2		
13a	RSBR		

MSA, Middle Stone Age.
[a] Uncertain boundaries; see text for more detail.
[b] Less certain correlation; see text for more detail.

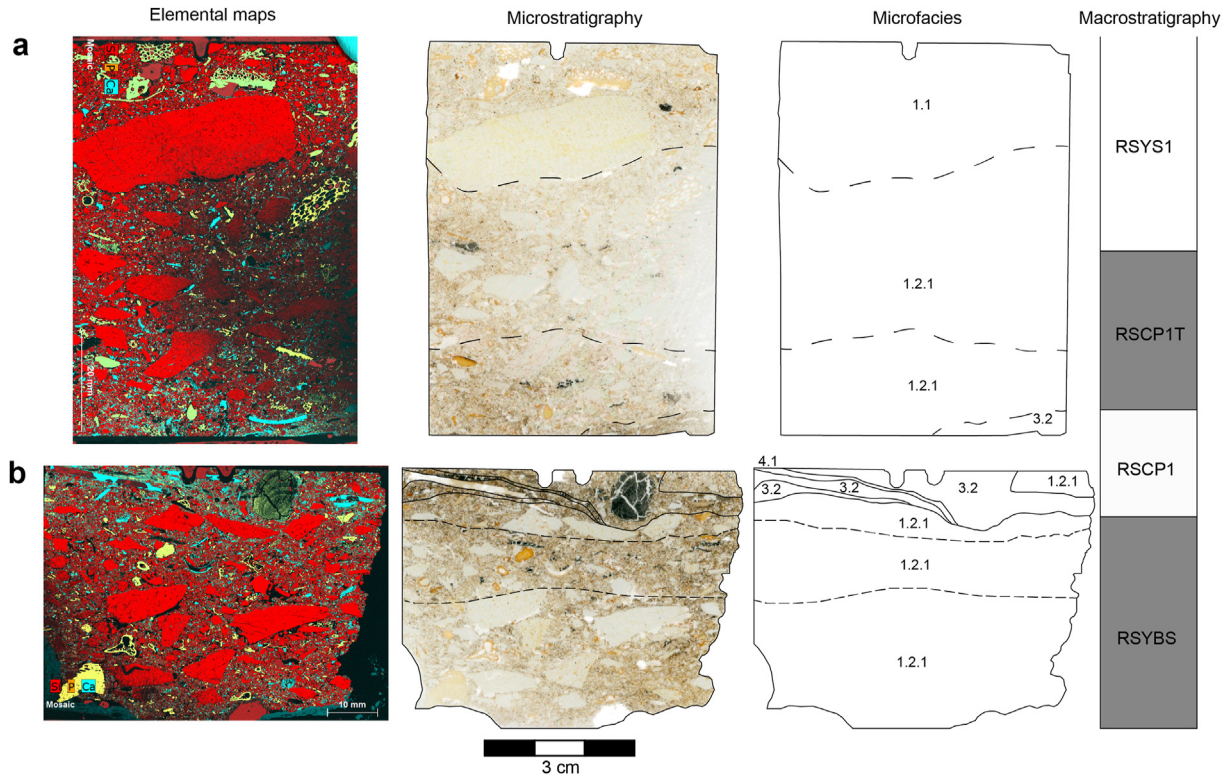

Figure 9. The micro-X-ray-fluorescence elemental maps, microstratigraphy, microfacies attributions, and excavation unit correlations (macrostratigraphy) for slides A (top row) and B (bottom row) from KRM-13-12. On the elemental maps blue denotes calcium (mostly ash or shell) and red represents silicon in the form of quartz and quartzite. Yellow shades show the presence of both calcium and phosphorus, e.g., in bone, phosphatized ash, and apatite nodules. (For interpretation of the references to color in this figure legend, the reader is referred to the web version of this article).

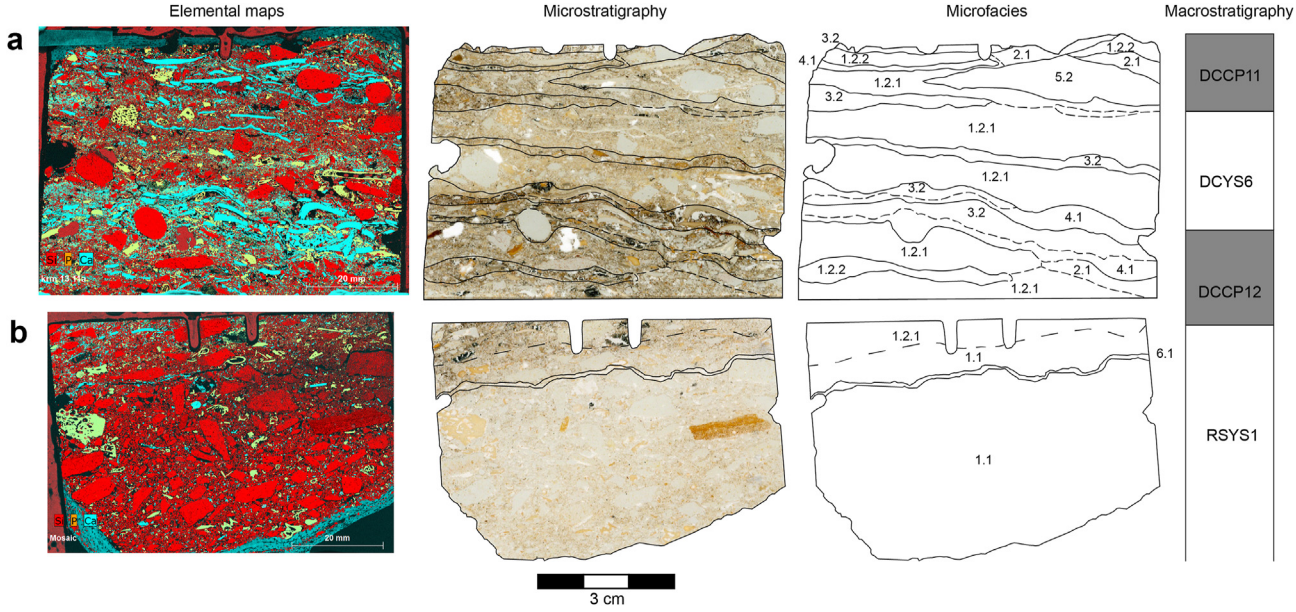

Figure 10. The micro-X-ray-fluorescence elemental maps, microstratigraphy, microfacies attributions, and excavation unit correlations (macrostratigraphy) for slides A (top row) and B (bottom row) from KRM-13-11. On the elemental maps blue denotes calcium (mostly ash or shell) and red represents silicon in the form of quartz and quartzite. Yellow shades show the presence of both calcium and phosphorus, e.g., in bone, phosphatized ash, and apatite nodules. (For interpretation of the references to color in this figure legend, the reader is referred to the web version of this article).

The unit RSCP1T includes one MSU and part of another (Fig. 9). Both are ashy sands with a significant quartzite component (MF 1.2.1), but the lower deposit is notably ashier and contains more charcoal. Shell fragments are common but seldom more than a few mm in length. Bone is also common, ranging from sand-sized to ~9 mm. There is a significant increase in the size of the quartzite fragments moving up through the unit. The transition to RSYS1 is diffuse, and thus, the depiction in Figure 9 is an approximation.

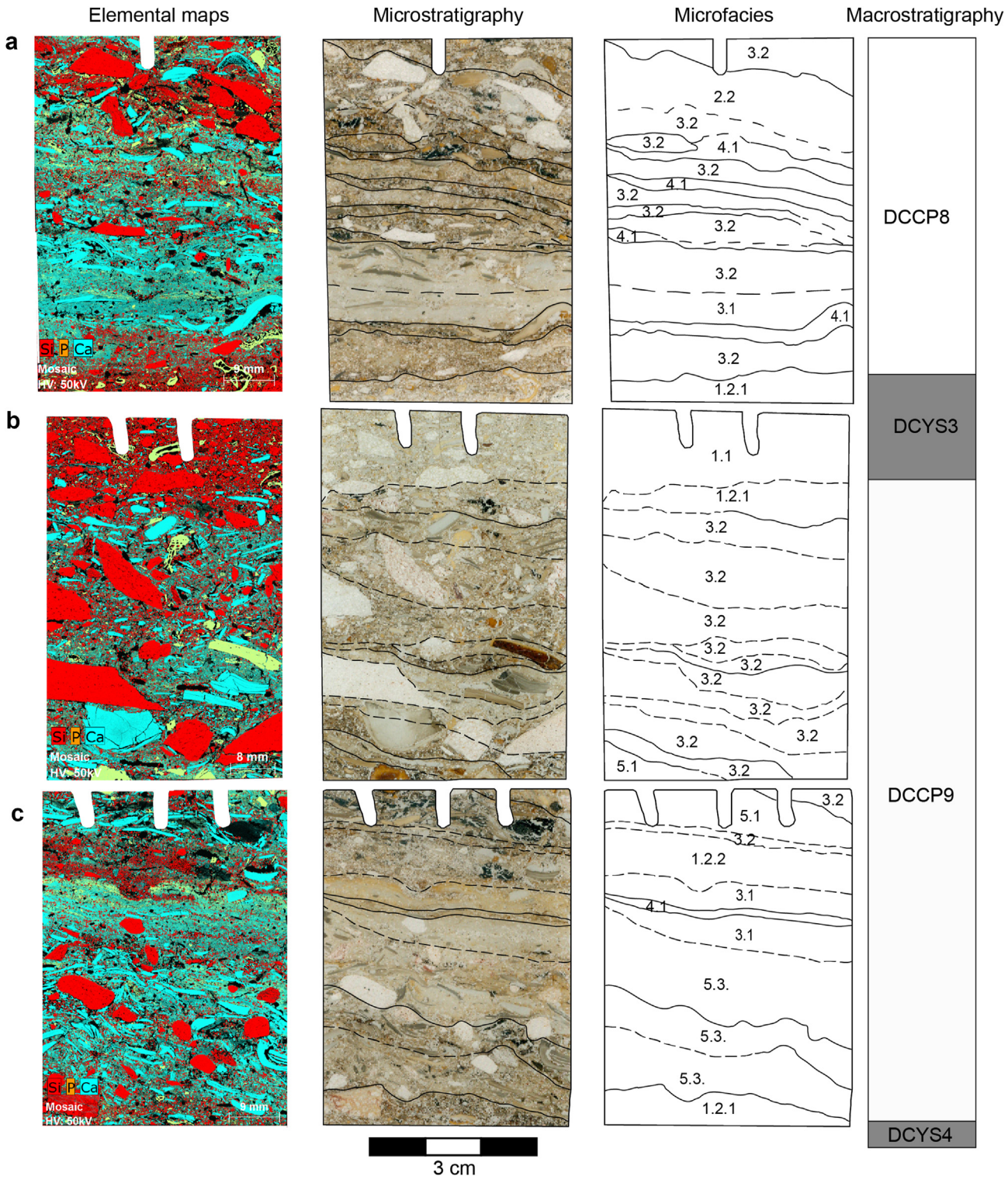

Figure 11. The micro-X-ray-fluorescence elemental maps, microstratigraphy, microfacies attributions, and excavation unit correlations (macrostratigraphy) for slides A (top row), B (middle row), and C (bottom row) from KRM-13-10. On the elemental maps blue denotes calcium (mostly ash or shell) and red represents silicon in the form of quartz and quartzite. Yellow shades show the presence of both calcium and phosphorus, e.g., in bone, phosphatized ash, and apatite nodules. (For interpretation of the references to color in this figure legend, the reader is referred to the web version of this article).

The slightly ashy sand deposit (MF 1.2.1) at the base of RSYS1 is overlain by several sandy MSUs (Figs. 9 and 10). These deposits, assigned to MF 1.1, have a very high concentration of angular quartzite fragments, which range in size from coarse sand to several cm in length. Shell fragments, including sand-sized pieces, are relatively limited and are seldom larger than a few mm (note

Table 5
The microfacies identified in the samples from square PP38, Cave 1B. A general description is provided for each microfacies, along with a list of the excavation units/unit groups in which they were recorded, and the number of microstratigraphic units assigned to the microfacies. See Figures. 12–14 for photomicrographs of each microfacies. All observed phosphatization of ash is by apatite.

No.	Microfacies	Description	Context
1	Shelly sand		
1.1	Shelly sand with quartzite	Matrix of predominantly sand-sized subangular to rounded grains of quartz and marine shell. Quartz significantly more common than shell. Angular fragments of quartzite ranging from coarse sand to several cm in length are very common. Rare larger quartzite clasts. Bones and bone fragments common, up to ~1 cm in length. Many appear to be microfauna. Larger elongated shell fragments far less common than bone. In situ breakage of bone and shell common but with very limited vertical displacement of pieces. Small secondary apatite nodules are present dispersed through the matrix and in a thin layer in one case (see text for further description).	RSYS1 (three MSUs) DCYS3 (one MSU)
1.2	Ashy shelly sand with coarser inclusions		
1.2.1	—with quartzite	Shelly sand as defined earlier but with a greater concentration of shell. Ash fills the interstitial space to varying degrees. Angular quartzite fragments with size ranging from coarse sand to pebble-sized are common. Both the size and density of quartzite vary within and between MSUs. Elongated shell fragments up to ~4 cm in length, but mostly under 1 cm, are present in many of these deposits but are never very common. Bone, including microfauna, is more common than shell, but has a similar size range. Charcoal fragments under 1 cm were observed in some deposits, whereas fine charred organic material was more common but still a relatively minor component. Some in situ breakage of shell but very limited vertical displacement of fragments. Minor phosphatization of ash common.	RSYBS (three MSUs) RSCP1 (one MSU) RSCP1T (two MSUs) RSYS1 (one MSU) DCCP12 (three MSUs) DCYS6 (two MSUs) DCCP11 (one MSU) DCYS4 (one MSU) DCCP9 (one MSU) DCYS3 (one MSU)
1.2.2	—without quartzite	Sand and ash matrix as in MF 1.2.1. Larger elongated shell fragments (<1 cm) and some more equant pieces are relatively common, and bone ranging in size from coarse sand to granule/pebble is present but less common. Charcoal up to ~5 mm observed in some MSUs. Some finer charred organic material distributed through the ash. Pockets of minor ash phosphatization. No visible in situ fragmentation of shell.	DCCP12 (one MSU) DCCP11 (two MSUs) DCCP9 (one MSU)
2	Quartzite gravel		
2.1	Fine sandy gravel with ash	Angular quartzite clasts all <1 cm in length in a matrix of shelly sand, with some ash filling the interstitial spaces. Small bone fragments and charred fine organic matter are present in some units, but relatively rare. The quartzite fragments all show a general preferred orientation which matches that of the respective MSU in both direction and degree of dip.	DCCP12 (one MSU) DCCP11 (two MSUs)
2.2	Fine ashy gravel with coarse inclusions	Angular quartzite clasts all <2 cm in length in a matrix of ash and shelly sand. Matrix-supported in some pockets. Some of the clasts resemble lithics in cross-section. One rounded clast also present. Relatively small shell and bone fragments present throughout the MSU. Some in situ breakage of bone and shell visible but with very limited vertical displacement of pieces. The quartzite fragments have a general preferred orientation which corresponds with the direction and degree of dip of the MSU itself. Minor phosphatization of ash throughout.	DCCP8 (one MSU)
3	Ash		
3.1	Microlaminated ash and sand	Ash with virtually no coarse inclusions, interbedded with microlaminae of shelly sand (often just a single sand grain in thickness) and extremely thin bands of phosphatized ash. Some variable recrystallisation and cementation of ash in this MF and all others with a significant ash component. Small channels are present at low frequency in some of the deposits.	DCCP9 (two MSUs) DCCP8 (one MSU)
3.2	Ash with sand and coarser inclusions	Ash-dominated deposits containing varying quantities of shelly sand. The presence, density, and size ranges of coarser inclusions vary widely between the MSUs assigned to this MF. Quartzite ranges from angular coarse sand to granule-sized fragments and clasts several cm in length. Many, but not all, of the latter are either rounded pebbles or have cross-sections suggestive of being lithics. Bone fragments are relatively common in many MSUs, but are generally quite small, seldom exceeding 4 mm in length. Shell fragments are typically elongated, and few are more than 1 cm in length. Charcoal pieces under 1 cm are present in some deposits, and fine charred material is found within the ash matrix of some MSUs. The dip and orientation of the coarser inclusions typically corresponds roughly with that of the MSU they are in. In situ breakage of shell is common where shell is present, but vertical displacement of the fragments is relatively limited. Phosphatization of ash is very common but varies in intensity. It is often patchy, but sometimes there are extremely thin lenses of phosphatized	RSCP1 (three MSUs) RSCP1 (one MSU) DCCP12 (two MSUs) DCYS6 (one MSU) DCCP11 (one MSU) DCCP9 (11 MSUs) DCCP8 (9 MSUs)

(*continued on next page*)

Table 5 (*continued*)

No.	Microfacies	Description	Context
		ash within ash that is either not phosphatized or less phosphatized. Small channels are present at low frequency in some of the deposits.	
4	Organic material		
4.1	Charred organic material	Fine charred organic material and charcoal with ash and some shelly sand filling spaces between charred material and other inclusions. Larger elongated shell fragments (up to ~9 mm) are common, while sand to granule-sized bone is also present, but less common. Minor phosphatization of ash and charcoal in some MSUs of this microfacies. In situ fragmentation of shell is variable.	RSCP1 (one MSU) DCCP12 (two MSUs) DCCP11 (one MSU) DCCP9 (one MSU) DCCP8 (four MSUs)
5	Shell		
5.1	Shell with charred organic material	Shell fragments <2 cm in length (mostly elongated) with a matrix of ash and some shelly sand. Charcoal fragments up to ~9 mm are common, along with some finer charred organic material within the ash. In situ breakage of shell common, but with limited vertical displacement of fragments. Minor phosphatization of ash throughout. The shell fragments typically dip at a similar angle, and in the same direction, as the MSU itself.	DCCP9 (one MSU)
5.2	Shell with rounded quartzite	Shell fragments <2 cm in length (mostly elongated) with a matrix of ash and shelly sand. Some angular quartzite from coarse sand to granule-sized, and several relatively large (up to ~1 cm) rounded quartzite pebbles. Minor localized phosphatization of ash. Very little in situ fragmentation of shell visible. Dip of shell fragments largely corresponds to upper and lower surfaces of MSU.	DCCP11 (one MSU)
5.3	Ashy shell	A very high density of shell fragments up to ~1 cm long in an ash matrix. Both charcoal and finer charred organic material present but vary in concentration between different MSUs. Some shelly sand and sand-sized angular quartzite throughout, but there are clear concentrations in some areas. Larger quartzite pieces are mostly rounded. Some shell fragments appear to represent whole shells broken in situ with relatively limited vertical displacement. Small bone fragments present but not common. The shell and larger quartzite dip relatively steeply, matching the overall orientation of the deposits. Phosphatization of ash throughout but variable in degree.	DCCP9 (3 MSUs)
6	Calcite		
6.1	Micritic calcite	Thin, laterally continuous lamina of mostly micritic calcite, with some small areas of more microsparitic calcite. No visible clastic sediment within the calcite and internal stratification absent. Heavily affected by dissolution.	RSYS1 (one MSU)

Abbreviations: MF, microfacies; MSU, microstratigraphic unit.

the lack of calcium in these units in the elemental maps in Figs. 9a and 10b). In contrast, bone—including microfauna—is far more common and some pieces are more than 1 cm in length. Small secondary apatite nodules are present through the deposits. The sandy MSUs are interrupted only by a very thin layer (up to ~2-mm-thick) of micritic calcite (MF 6.1) with localized domains of more microsparitic calcite (Fig. 10). This deposit has been partially dissolved but can be tracked across the slide as a distinct accommodated planar void (Fig. 15). It is overlain by another MSU assigned to MF 1.1 which is notably less rich in quartzite and has generally smaller bone fragments than the deposits below. Clasts throughout RSYS1 show a general, but not particularly strong, tendency towards horizontality. In the upper MSU, however, there is an apparent line of quartzite fragments and bone within the sand just above the calcite. Above this, at the very top of the unit, small secondary apatite nodules form another rough line within the sandy matrix (Fig. 15).

DCCP12 is a group of units at the base of the DC deposits, which are the lowermost MSA II units in Cave 1B. It comprises two distinct portions, each containing multiple MSUs (Fig. 10). The lower portion includes five deposits of ashy sand with varying concentrations of quartzite, which are assigned to MFs 1.2.1, 1.2.2, and 2.1. Bone and shell fragments under ~5 mm are present at relatively low concentrations throughout, while charcoal is only present in the basal MSUs. Small secondary apatite nodules are scattered through a few of the deposits. The upper portion contains four alternating deposits dominated by charred organic material (MF 4.1) and ash (MF 3.2). Quartzite is fairly limited in quantity, but both bone and shell are present in high concentrations, especially in the ash-dominated deposits. The bone fragments are all under 1 cm, but some pieces of shell are several cm in length. In situ breakage of shell and bone is very common across the lateral extent of these deposits. Visible vertical displacement is limited, and many fragments appear to fit with surrounding fragments (Fig. 16). The general dip of the shell and bone matches that of the deposits themselves. Pockets of slightly phosphatized ash are common within both the lower and upper portions of DCCP12. In this case, and for all examples in the sampled deposits, the phosphatization was in the form of apatite replacing calcite.

DCYS6 (Fig. 10) is made up of a very thin deposit of sandy ash with bone and charred organic material (MF 3.2) sandwiched between two deposits of slightly ashy sand (MF 1.2.1). The lower is notably richer in bone and quartzite, whereas the upper contains more shell.

The DCCP11-unit group has a thin, discontinuous ash-dominated deposit (MF 3.2) at its base (Fig. 10). Most of the rest of the unit is comprised of ashy sand with varying concentrations of quartzite and shell. This includes an MSU with some quartzite assigned to MF 1.2.1, two with virtually no quartzite (MF 1.2.2), and two with highly concentrated quartzite (MF 2.1). A wedge-shaped deposit rich in shell and rounded quartzite pebbles (MF 5.2) makes up a significant portion of the unit. Some in situ breakage of shell was observed, with limited displacement of fragments. A lens of sediment rich in charred organic material (MF 4.1) also wedges out within the predominantly sandy unit. An extremely thin layer of sandy ash (MF 3.2) with small coprolites is the uppermost MSU

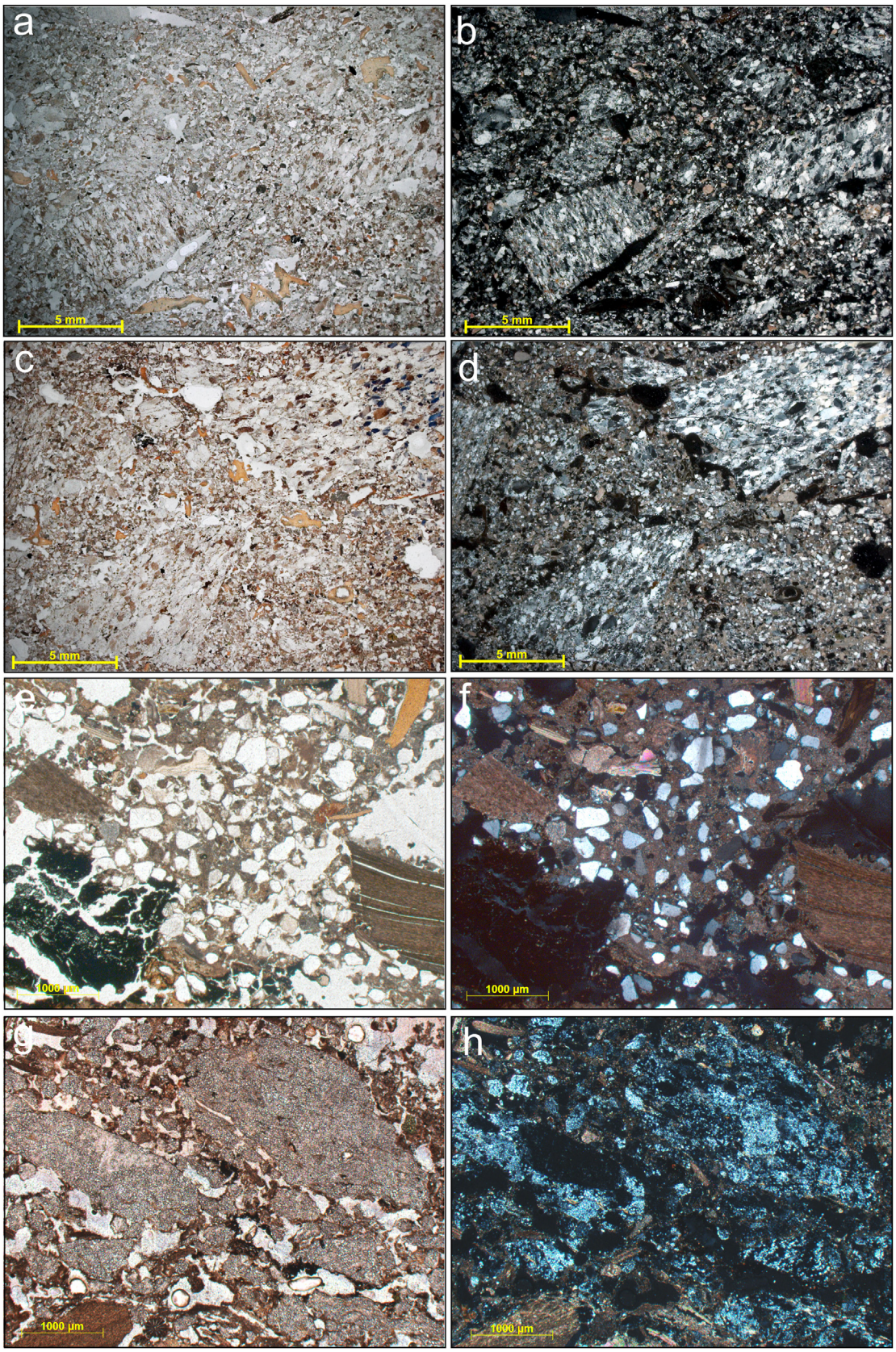

Figure 12. a) Sand-sized quartz, quartzite, and shell with angular quartzite gravel and bone fragments (microfacies [MF] 1.1), plane-polarized light (PPL). b) Same as a, cross-polarized light (XPL). c) Shelly sand with ash, charred material, angular quartzite gravel, and bone fragments (MF 1.2.1), PPL. d) Same as c, XPL. e) Shelly sand with ash, charred material, and shell and bone fragments (MF 1.2.2), PPL. f) Same as e, XPL. g) Quartzite gravel with shelly sand, ash, and charred organic material (MF 2.1), PPL. h) Same as g, XPL. Note that the colors (especially for quartzite) differ from normal because the pictured area of this slide was ground relatively thin.

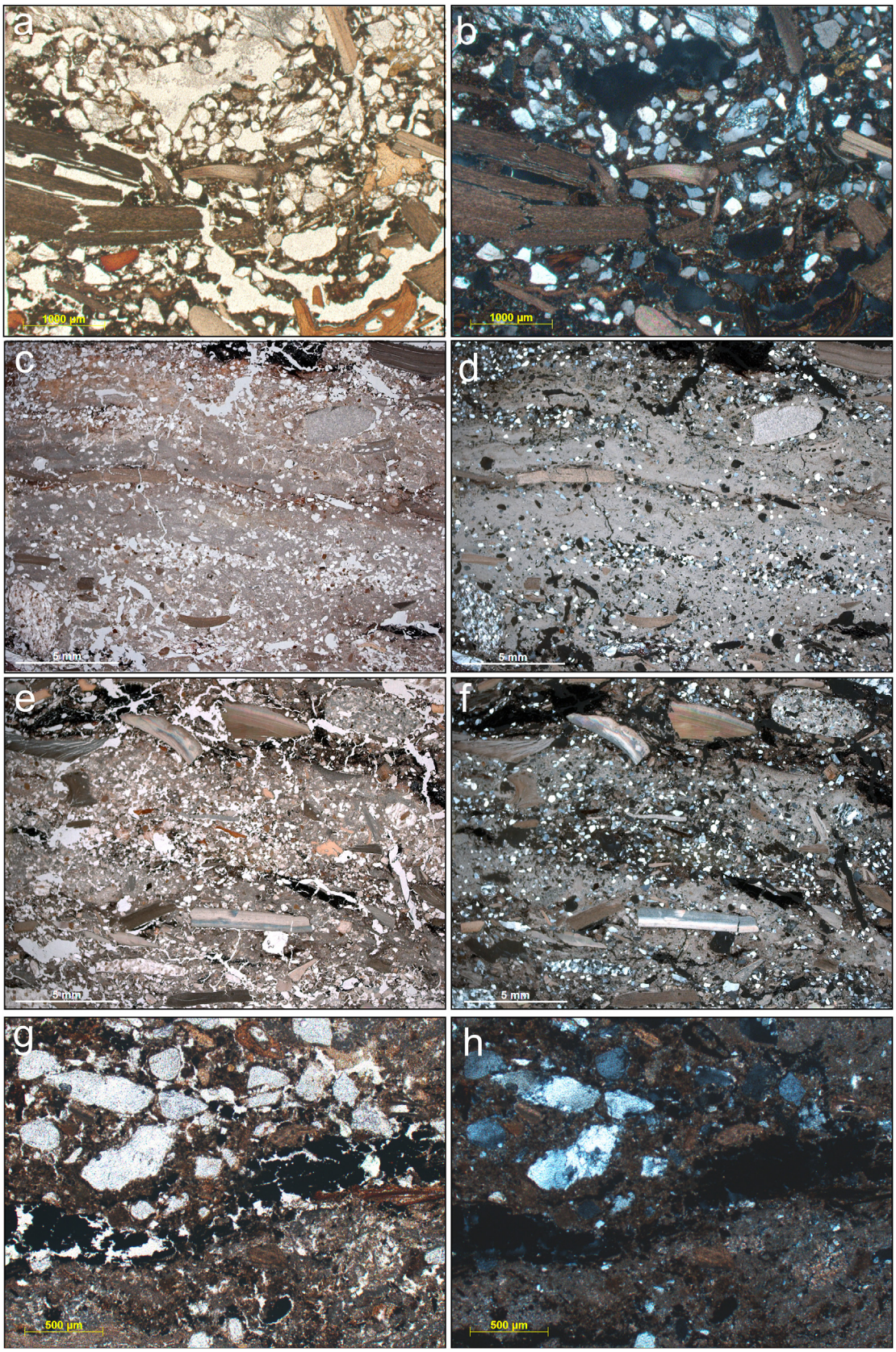

Figure 13. a) Quartzite gravel in an ash matrix, with shell, sand, and bone and shell inclusions (microfacies [MF] 2.2), plane-polarized light (PPL). Note contact with underlying ash-dominated deposit. b) Same as a, cross-polarized light (XPL). c) Microlaminated ash with phosphatized bands and very thin sand laminae (MF 3.1), PPL. Note the scarcity of larger inclusions. d) Same as c, XPL. e) Multiple ash-dominated deposits with shelly sand and larger inclusions (MF 3.2), PPL. Note the variation in the type and proportion of inclusions, and the presence of lenses of charred material (MF 4.1) f) Same as e, XPL. g) A thin lens of charred organic material (MF 4.1) between two ash-rich deposits, PPL. h) Same as g, XPL.

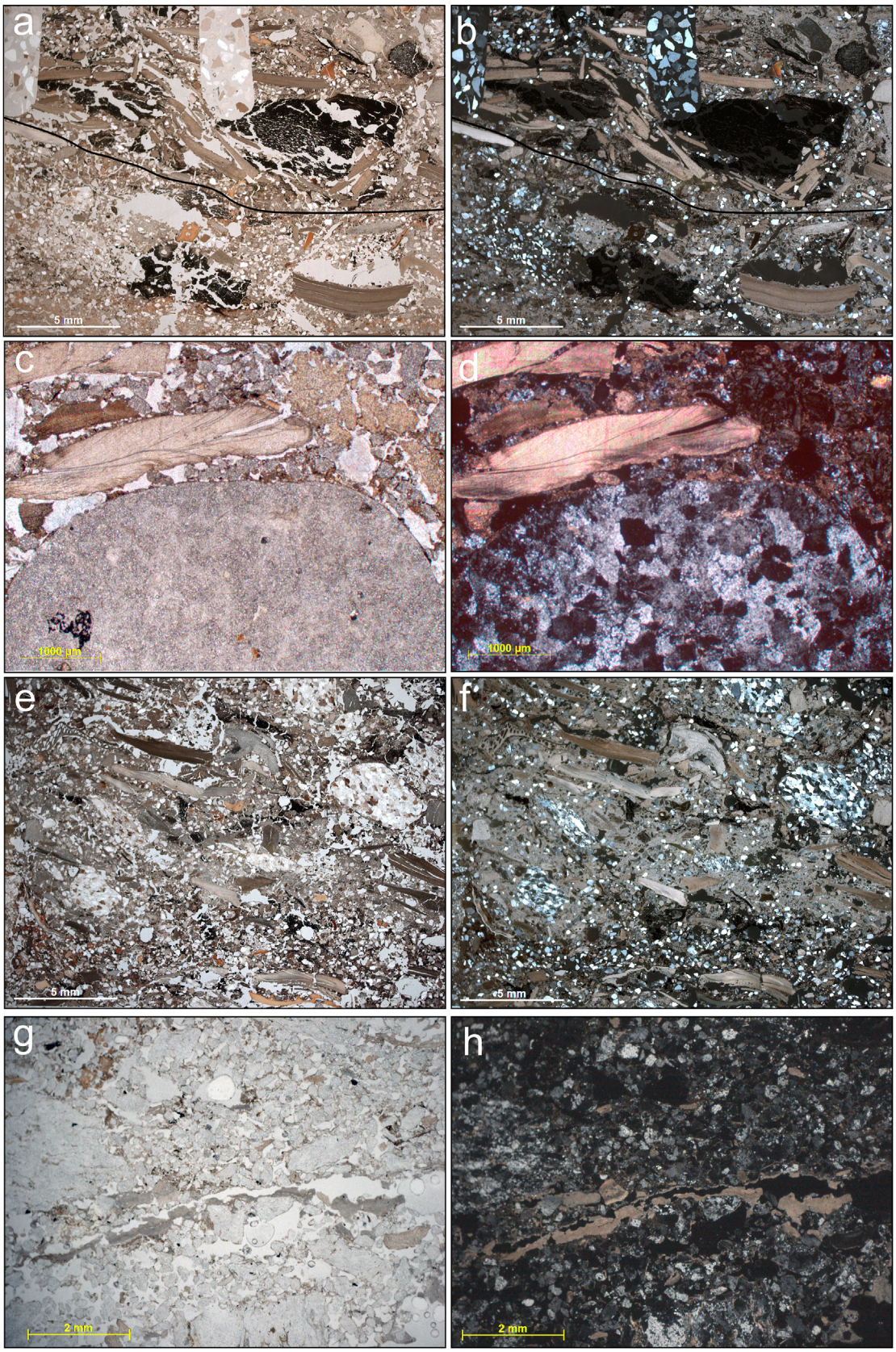

Figure 14. a) Above the line: shell and charred organic material, including charcoal, in a matrix of ash and shelly sand (microfacies [MF] 5.1), plane-polarized light (PPL). The deposit below the line is assigned to MF 1.2.2 The cuts into the deposit are a product of thin-section production, and the grains are unrelated to the original deposits. b) Same as a, cross-polarized light (XPL). c) Shell with relatively large, rounded quartzite in a matrix of shelly sand and some ash (MF 5.2), PPL. Note the crushed bone (upper right of the image). d) Same as c, XPL. e) Shell fragments in an ash matrix with charred material, bone fragments and shelly sand as inclusions (MF 5.3), PPL. The density of shell varies within and between MSUs of this type. Note the contact with the underlying MF 1.2.1 deposit. f) Same as e, XPL. g) Thin lamina of micritic calcite, with some more microsparitic zones (MF 6.1), PPL. Note the void within the calcite. h) Same as g, XPL.

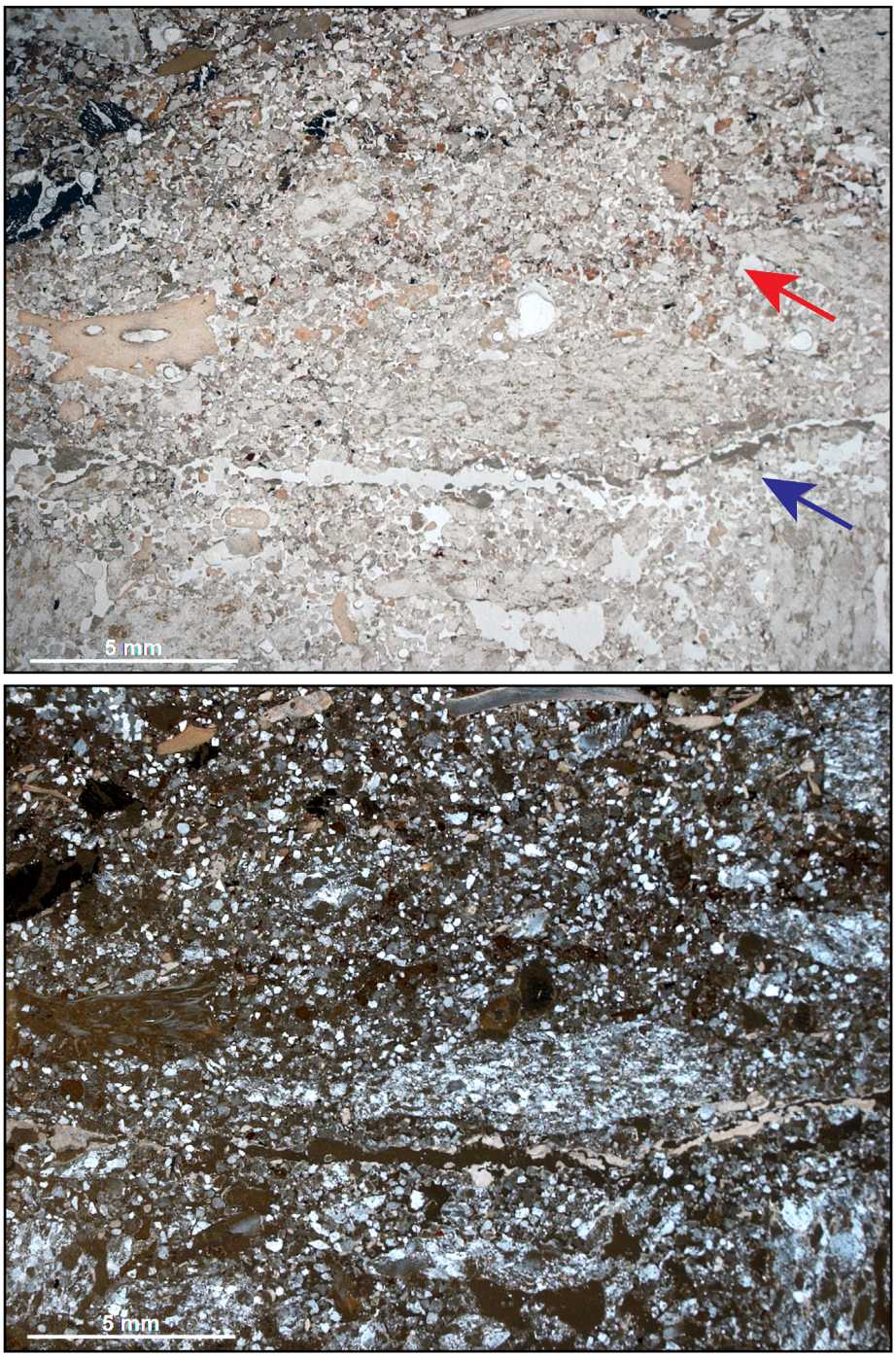

Figure 15. The upper portion of RSYS1 in plane-polarized light (top) and cross-polarized light (bottom). The calcite crust (microfacies 6.1.) is indicated with the blue arrow. Note the void due to dissolution. The red arrow indicates the line of apatite nodules. Most of the view is composed of microfacies 1.1 sediment. The appearance of anthropogenic materials (ash, charcoal, shell) above the apatite nodules marks the transition to DCCP12. (For interpretation of the references to color in this figure legend, the reader is referred to the web version of this article).

from DCCP11 represented in the samples. The ash is relatively highly phosphatized at the very top of the sample.

DCYS5 and DCCP10 both appear to have fallen between samples KRM-13-11 and KRM-13-10 and thus are not represented in the thin sections. This is not unexpected, as they are both extremely thin at this point in the northern profile.

DCYS4 is also very thin across the sampling column location and is represented by a single thin MSU (Fig. 11). This deposit of ashy sand (MF 1.2.1) contains a single relatively large quartzite clast and limited bone and shell fragments but is fairly rich in charred organic material, both as small charcoal fragments and finer material within the ash. Some small coprolites are spread through the unit. A portion of the contact with the overlying MSU is a lens rich in relatively highly phosphatized ash, concentrated apatite nodules, and containing a partially phosphatized shell fragment (rare for Cave 1B; Fig. 17). This lens lies directly on the quartzite clast but appears to have been deformed next to the clast, wrapping along the side of the clast, before flattening out somewhat moving away

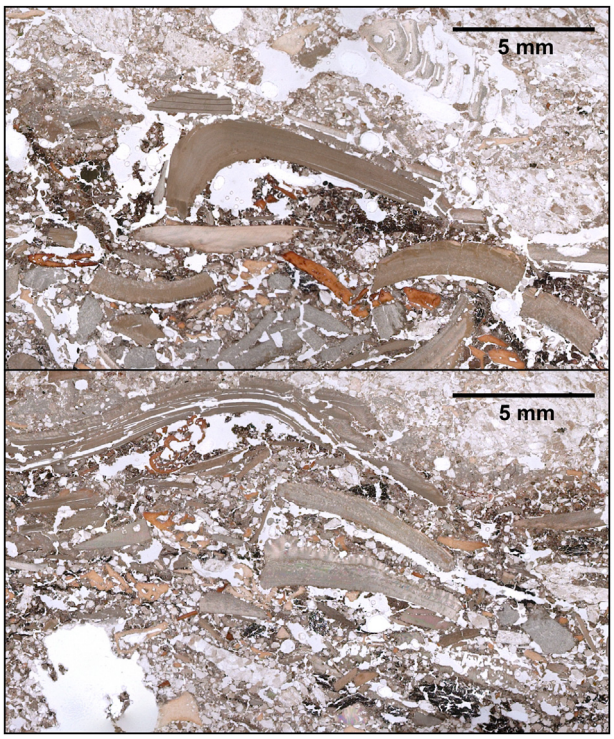

Figure 16. Two views of the upper portion of DCCP12 (plane-polarized light). Note the general horizontality and limited displacement of bone and shell fragments.

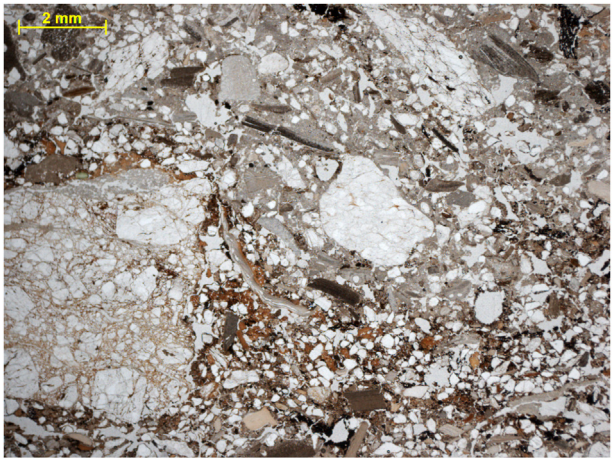

Figure 17. The contact between DCYS4 (microfacies 1.2.1) and the overlying microfacies 5.3 within DCCP9, showing the deformed lens of apatite above and next to the quartzite clast (plane-polarized light). Note the nearly vertical partially phosphatized shell fragment, and the conformity of the base of the overlying ash to this surface.

from the clast. The base of the overlying ashy MSU is conformable to this surface.

The unit group DCCP9 is a relatively thick package of mostly ash-dominated deposits (Fig. 11). Its base is made up of three relatively steeply dipping MSUs assigned to MF 5.3, which are rich in large shell fragments and rounded quartzite pebbles within an ash matrix. Sand and some smaller angular quartzite fragments are present but occur at their highest concentration just above the bulk of the shell. Charred organic material is concentrated in the middle of the three MSUs, with little in the other two. Minor ash phosphatization is common. There is some in situ fragmentation of shell, most notably at the upper surfaces of the two lower MSUs. These

Figure 18. The contact between laminated ash (microfacies 3.1) and ashy sand (microfacies 1.2.2) within DCCP9 (plane-polarized light). Note the truncation of the ash by a channel-like feature (red arrow) and the bands of yellowish phosphatized ash (black arrows). (For interpretation of the references to color in this figure legend, the reader is referred to the web version of this article).

deposits are overlain by two laminated MSUs of ash, phosphatized ash, and sand lenses (MF 3.1) separated by a thin layer rich in charred organic material (MF 4.1). The laminated ash contains virtually no inclusions larger than sand. The upper contact of the laminated ash is an unconformity, with the overlying deposit filling a hollow in the surface (Fig. 18). This deposit is mostly ashy sand (MF 1.2.2) but varies laterally with some ash-dominated domains, which contain most of the shell and charcoal in this MSU. It is capped by a very thin layer of sandy ash (MF 3.2), which is overlain in turn by a shell-rich deposit with an ashy matrix, significant charcoal content, and a single relatively large bone (MF 5.1). Shell fragmentation is particularly common in this MSU, but the displacement is limited, and most fragments can be associated with other fragments from the same shell. This deposit is followed by a sequence of 10 MSUs, which are all assigned to MF 3.2 but vary in the concentration of different inclusions. The first seven contain some sand and a few large pieces of bone, shell, and quartzite. Charred organic material (both fine and some charcoal) is concentrated in a few of the MSUs. The next two MSUs are richer in sand and smaller quartzite fragments, with notably smaller bone and shell fragments than below. Charred organic material is limited. The uppermost of the MF 3.2 MSUs is rich in shell, with some bone and small quartzite fragments. Some shell has been fragmented in situ, with very little displacement of fragments. Minor phosphatization of ash is common through these 10 MSUs, sometimes present in the form of extremely thin lenses. The final MSU within DCCP9 is a deposit of ashy sand with charcoal, shell, and quartzite (MF 1.2.1).

Unit DCYS3 comprises two sandy MSUs (Fig. 11). The lower contains a high concentration of angular quartzite, bone (including microfauna), and some shell. Sand-sized shell fragments are rare (note the lack of calcium in this deposit in the elemental map in Fig. 11b). It is assigned to MF 1.1, whereas the upper MSU is ashy enough to fall within the characteristics of MF 1.2.1. Shell and quartzite are both less common in this deposit than in the lower one.

DCCP8 is the uppermost unit group represented in the samples (Fig. 11). As with DCCP9, it is primarily made up of ash-dominated deposits. The basal deposit is ash with some sand and relatively fine quartzite (MF 3.2), which grades laterally into a sandier sediment with larger quartzite pieces and bone (MF 1.2.1). Most of the rest of the unit is characterized by an alternating sequence of deposits rich in charred organic material (MF 4.1) and ash-

dominated layers (MF 3.1 and 3.2). The first organic-rich MSU contains relatively dense shell, which has been relatively heavily fragmented in situ, with very little displacement. This deposit is overlain by an MSU of laminated ash, phosphatized ash, and sand (the only example of MF 3.1 in this unit), followed by an ash deposit rich in shell with some sand and quartzite. Some of the shell in the upper of these MSUs may have been pressed into the ash, and there are indications of in situ breakage with limited displacement. The second carbon-rich MSU contains few coarse inclusions and is followed by a succession of three ash-dominated deposits. The lowermost is rich in shell, and contains some sand and quartzite, including pieces that appear to be lithics. The second is richer in charred material but contains less shell, sand, and quartzite, whereas the third is sandier but has few coarser inclusions. The third charred organic MSU and the overlying ash-dominated deposit are both relatively rich in shell and sand, with rarer inclusions of very small bone and quartzite fragments. The ash in the ash-dominated deposit is more notably phosphatized than in any of the preceding MSUs in DCCP8. The fourth and final of the MSUs assigned to MF 4.1 is relatively rich in ash and contains shell and bone, along with larger charcoal pieces than in the preceding deposits. The ash in both this deposit and the two overlying ash-dominated MSUs is also relatively highly phosphatized. The uppermost ash contains shell, quartzite, charcoal, small pieces of bone, and a single rounded piece of calcarenite. This succession of alternating charred organic and ashy deposits is capped by a relatively steeply dipping deposit dominated by quartzite fragments and sand, with ash filling much of the interstitial space (MF 2.2). Shell and bone fragments are both reasonably common, and some charcoal is visible. The final MSU in the sampled sequence is ash with sand, shell, bone, and very small quartzite fragments (MF 3.2). Some in situ fragmentation of shell is visible, and a round piece of shell appears to have been pressed down into the ash near the base of the deposit.

Table 6
The interpretation of the microfacies identified in the sampled deposits in PP38, Cave 1B. Note that phosphatization of ash is by apatite.

No.	Microfacies	Interpretation	Geo.	Bio.	Anth.
1	Shelly sand				
1.1	Shelly sand with quartzite	Deposition through aeolian and/or colluvial processes (sand) and breakdown of the host rock (angular quartzite clasts), with the latter mostly driven by salt weathering. Bone (much of it microfauna) and shell introduced by marine birds, raptors, and small mammal carnivores. Secondary apatite nodules formed by biogenic apatite. Possible incomplete decalcification due to acidic phosphates.	x	x	
1.2	Ashy shelly sand with coarser inclusions				
1.2.1	—with quartzite	Predominantly geogenic deposits containing material reworked from combustion features, trampling probably a significant process. Some biogenic input in the form of bone, shell, and alteration of ash by secondary apatite.	x	x	x
1.2.2	—without quartzite	Very similar to 1.2.1, but lack of quartzite suggests either slower host rock breakdown or more rapid accumulation of deposit.	x	x	x
2	Quartzite gravel				
2.1	Fine sandy gravel with ash	Similar to MF 1.2.1 but thinness and significantly greater quartzite content indicate winnowing after deposition, most likely by localized low energy surface water flows.	x		x
2.2	Fine ashy gravel with coarse inclusions	Similar to MF 1.2.1 but with a greater concentration of reworked anthropogenic components. Some evidence for trampling but perhaps prior to final deposition. Alteration by biogenic secondary apatite.	x	x	x
3	Ash				
3.1	Microlaminated ash and sand	Intact hearths, with laminae of sand and phosphatized ash suggesting multiple burning events in the same location. The alteration of ash by secondary calcite and apatite, and minor bioturbation by soil mesofauna are the only obvious post-depositional processes.	x	x	x
3.2	Ash with sand and coarser inclusions	Combustion features that have been reworked to varying degrees. Some still clearly identifiable as hearths with inclusions of food debris or lithics. Trampling and alteration by secondary calcite and apatite common. Some minor bioturbation by soil mesofauna.	x	x	x
4	Organic material				
4.1	Charred organic material	Incomplete combustion of organic material at the base of hearths. Bone and shell either fuel/discard or chance inclusions from pre-existing surface. Minor alteration of ash and charcoal by apatite.	x	x	x
5	Shell				
5.1	Shell with charred organic material	Incomplete combustion of organic material on top of shell. Deposit trampled and altered by secondary apatite.	x	x	x
5.2	Shell with rounded quartzite	Reworking and mixing of ash, sand, and shell-rich deposits which could have been small middens. Some trampling likely involved in this process. Some ash altered by biogenic secondary apatite.	x	x	x
5.3	Ashy shell	The product of the mixing of originally more distinct shell and ash deposits, or the reworking of a combined ash and shell midden. The size of the shell fragments, and evidence for in situ fragmentation, suggest trampling likely played a role in this mixing. Sand (comprising both shelly sand and angular quartzite coarse sand) mixed into the deposits was likely originally present in distinct geogenic lenses. The secondary apatite that altered some ash was biogenic in origin.	x	x	x
6	Calcite				
6.1	Micritic calcite	Precipitation of calcite from calcium enriched water on the surface to form a crust during a hiatus in clastic deposition. Partial dissolution by relatively acidic water.	x		

Abbreviations: Geo., geogenic; Bio., biogenic; Anth., anthropogenic; MF, microfacies.

4. Discussion

4.1. Microfacies interpretation

The interpretations of the processes responsible for forming each of the MFs are discussed here and summarized in Table 6.

Shelly sand There are three MFs dominated by shelly sand in the sampled sequence: 1.1, 1.2.1, and 1.2.2 (Table 5). The sand component at KRM has been attributed to two primary sources: beach or dune sand transported and deposited by aeolian processes, and colluvial deposition of sand weathered from the Geelhoutboom palaeodune overlying the quartzite host rock (Deacon and Geleijnse, 1988). As both sources comprise sand-sized quartz and shell fragments, it is likely that the shelly sand in any specific MSU is from one or both of these sources.

Angular quartzite fragments ranging from coarse sand to pebble-sized are also a significant component of many of the MFs. Some pieces appear to be lithic debitage, but the majority are fragments of host rock. Given the climatic and geological context of the site, salt weathering would have played more of a role in the production of angular quartzite sand and gravel than frost-spalling (Miller et al., 2013, 2016), but insolation likely made some contribution to shelter breakdown (Butzer, 1982; Deacon and Geleijnse, 1988).

MF 1.1 is dominated by these geogenic components, but there are also inclusions of biogenic origin. The bone (much of it microfauna) and shell fragments were most likely deposited by birds and small mammals that utilized the shelter and the cliff above, whereas the small secondary apatite nodules are the product of the breakdown of phosphate-rich bird guano and subsequent reprecipitation of apatite within the groundmass (Karkanas, 2017). The relatively low proportion of sand-sized shell fragments in comparison to other deposits containing shelly sand suggests that some decalcification took place (e.g., Goldberg, 2000). The decomposition of guano can significantly lower pH levels, leading to the potential dissolution of calcite—with significant impacts on the preservation of ash, shell, and bone (e.g., Schiegl et al., 1996; Weiner et al., 2002). In this case, the presence of some shell and bone shows that this decalcification was not total.

MFs 1.2.1 and 1.2.2 are both dominated by shelly sand but also contain significant quantities of anthropogenic materials. The incorporation of wood ash, charred organic material, bone, and shell suggest the reworking of combustion features into largely geogenic deposits. Trampling is likely to have played a significant role in reworking the anthropogenic components (e.g., Goldberg et al., 2009; Miller et al., 2013; Rentzel et al., 2017). Raking or sweeping out of hearths could also have contributed to redistributing these materials, but no direct evidence for this behavior (e.g., Miller et al., 2010; Mallol et al., 2013a) was observed. Some bone, particularly microfauna, and shell is likely biogenic in origin, as is the apatite which has altered the ash in places. The presence and absence of quartzite is the major difference between these two MFs, reflecting a difference in host rock breakdown and/or in the rate at which a deposit was accumulated.

Quartzite gravel The composition of the thin, sloping MF 2.1 deposits suggests a broadly similar depositional process to MFs 1.2.1 and 1.2.2—primarily geogenic with some reworked anthropogenic material with trampling likely being a significant factor. In all cases, they have lateral and/or vertical contacts with MSUs assigned to MFs 1.2.1 or 1.2.2. The dominance of coarse sand to granule-sized quartzite over shelly sand and the relatively limited extent of these MSUs suggest that they could be lag deposits produced by the winnowing of finer material, perhaps by very localized low-energy surface water movement.

The single sloped deposit assigned to MF 2.2 contains significant quantities of both geogenic (shelly sand and angular quartzite) and anthropogenic components (ash, bone, shell, charred organic matter, and lithic artifacts). It is broadly similar to MF 1.2.1 but contains far more ash and more concentrated quartzite. The morphology of the deposit conforms to the surface of the seemingly truncated deposit beneath it, with the clasts showing the same general dip (Fig. 11). This deposit is interpreted as the product of the mixing of the geogenic components with lithic artifacts and material reworked from combustion features. The shell fragment size and angularity point to trampling as a possible process (Rentzel et al., 2017). The secondary apatite that altered patches of the ash is biogenic in origin (Karkanas, 2017).

Ash The ash in MF 3.1 is the product of complete combustion of wood (Canti and Briochier, 2017). The almost complete lack of coarse inclusions, and the common association with underlying deposits rich in charred organic material (MF 4.1) indicate that these MSUs are intact hearths (Mentzer, 2014; Mallol et al., 2017). The extremely thin sand laminae and slightly thicker bands of phosphatized ash suggest that each deposit is the result of repeated burning events at the same location. The sporadic recrystallization and cementation of ash by secondary calcite in this MF and other ash-rich deposits is a common phenomenon driven by water percolation through deposits (Karkanas et al., 2007; Karkanas, 2021). It is also possible that some secondary calcite was introduced by calcium-enriched water—as is the case across the rest of the complex (Deacon and Geleijnse, 1988; Wurz et al., 2022). The few small channels in the ash point to limited bioturbation by burrowing soil mesofauna (Stoops, 2021).

The dominance of ash, regular inclusion of charred organic material, and common association with deposits of MF 4.1 all indicate that MSUs assigned to MF 3.2 can be considered combustion features. However, the other inclusions suggest varying degrees of modification or reworking of these features but notably less than MFs 1.2.1 and 1.2.2 (Mallol et al., 2017). Apart from shelly sand and some quartzite (especially the coarse sand to granule sized pieces), the inclusions are anthropogenic in origin. Some could have been deliberately discarded into hearths both during and after burning events, but many were probably mixed into the ash after having been initially deposited in distinct layers. The shell fragments in some deposits are very small, and quite angular, and many of the larger fragments have experienced some in situ breakage (although typically with very limited vertical displacement of pieces). This, along with the mixing of sand and coarser material into the ash suggests that trampling played at least some role in the modification of these combustion features. As with MF 3.1, the ash has been altered by both secondary calcite and secondary apatite, although the latter tends to be relatively patchy, with lenses and lamina of phosphatized ash much less common and restricted to relatively intact hearths. The limited impact of burrowing soil mesofauna is evident from the rare small channels in some deposits.

The phosphatization of ash deposits in cave and rock shelter settings has been attributed to the decomposition of bird and bat guano (e.g., Karkanas et al., 2000; Karkanas, 2017). Cave 1B is relatively exposed, so bats are unlikely to have contributed guano, but marine birds have been observed roosting on ledges directly above the shelter. Their fish-dominated diet means their droppings are particularly rich in phosphorus, and the leaching and reprecipitation of the apatite produced by the alteration of the guano has even been known to phosphatize limestone (Glenn et al., 1994:758).

The bands of phosphatized ash within some combustion features (e.g., Fig. 18) are indicative of the exposure of these features

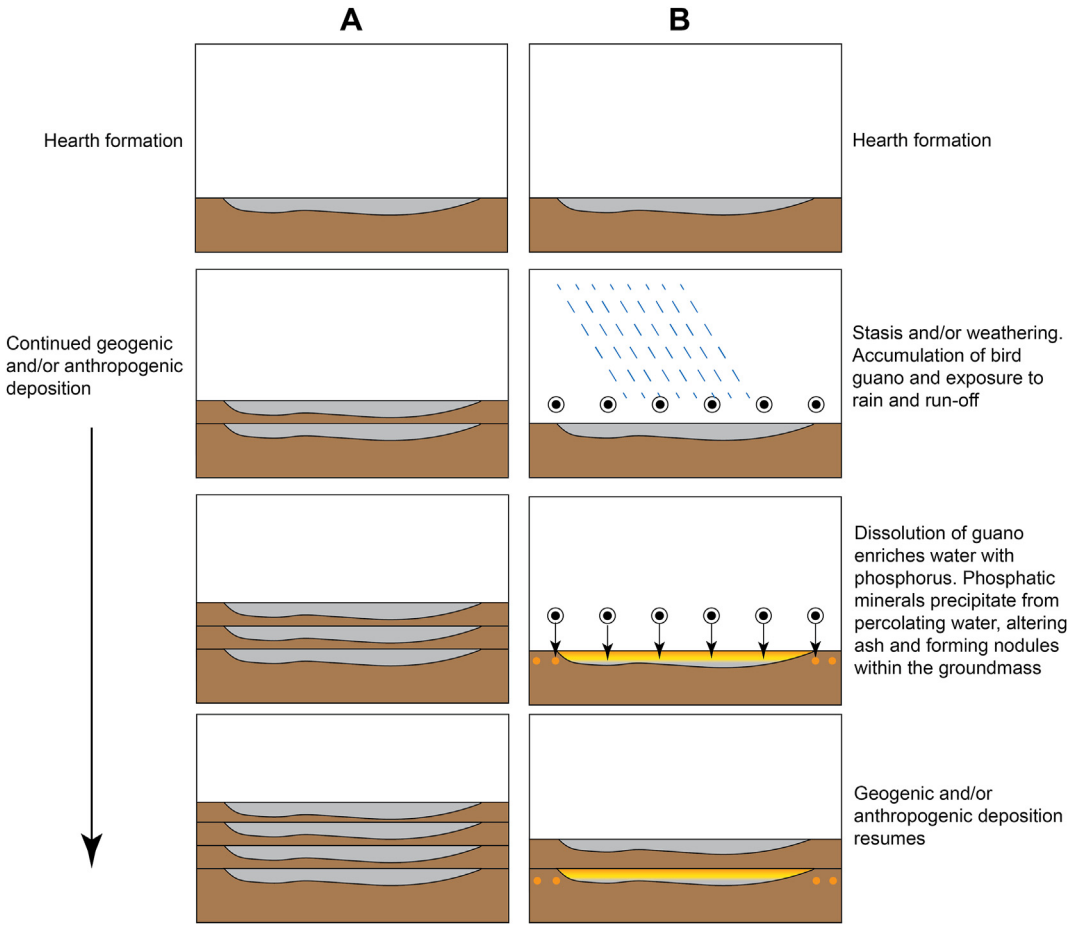

Figure 19. A comparison between A) hearths buried by continued deposition soon after their initial formation and B) hearths exposed on the surface for extended periods due to erosion or lack of deposition, leading to the alteration of the ash by biogenic secondary apatite. The secondary apatite can also precipitate into non-ash groundmass, forming nodules, but this is less common in the sampled sequence. Examples of both phosphatized and non-phosphatized hearths are preserved in the sampled sequence.

on the surface for a period of time due to erosion or a depositional hiatus (Fig. 19). The localized phosphatization points to a period of surface stability during which the ash was altered. The absence of phosphatized surfaces in some combustion features indicates that these were buried relatively quickly by natural or cultural deposits. The presence of ash, shell, and bone in the sampled combustion features and the relatively limited phosphatization of the ash suggest that this process was not a significant diagenetic process for these deposits. This stands in stark contrast to Cave 2, where some ash layers have been fully replaced by apatite, and all carbonates have been dissolved in one area of the cave (Wurz et al., 2022). The limited effects of phosphates on the sampled sequence may be due to either a comparatively low presence of guano or through calcite-rich water buffering the pH.

Most of the combustion features that can be interpreted as in situ hearths are stacked hearths (Figs. 18 and 20a), the product of multiple burning events in the same location (Mentzer, 2014). In some stacked sequences, the ash deposits are separated by charred layers of varying thickness (Mentzer, 2014: fig. 8e), but in others, charred layers are absent (Mentzer, 2014: fig. 8h), and different ash deposits are distinguished by phosphatized surfaces or extremely thin sand lenses. Single hearths (Fig. 20b) are notably less common. Charred organic material MF 4.1 is always overlain by ash deposits assigned to either MF 3.1 or 3.2. This association and the dominance of charcoal and fine charred organic material indicate that this MF is the product of incomplete combustion at the base of hearths (Mallol et al., 2017). The presence of shell and bone suggests that these materials were either deliberately placed in the fire as fuel or as discard or that they were already present on the surface when the fire was made and were thus incorporated into the base of the hearth (Mallol et al., 2013b). There is a minor biogenic input through the limited phosphatization of both ash and charcoal.

Shell The single deposit assigned to MF 5.1 shares similarities with that of MF 4.1 but contains significantly more shell. This deposit is interpreted as the base of a hearth, where the fire was made on top of a few shells, which were then covered by the charred organic material and ash that accumulated at the base of the hearth (Mallol et al., 2013b). The shell has fragmented in situ, although with little vertical displacement of fragments, suggesting that the deposit has been trampled (Villagran, 2019). Bird guano is the source of the secondary apatite which altered the ash in patches.

There are some similarities between the single MSU assigned to MF 5.2 and the three grouped into MF 5.3, but the former is far sandier and less ashy, and does not have the marked dip of the latter. MF 5.2 appears to be the product of the reworking and mixing of a midden-like deposit with sand and ash. The size and angularity of the shell suggests a mechanical process like trampling played at least some part in the formation of the deposit (Rentzel et al., 2017). MF 5.3 could potentially be the product of the mixing of shell midden layers with previously distinct ash and charred organic layers (either dumped material or reworked hearths) and geogenic lenses of sand and angular quartzite. Alternatively, it could represent the mixing of geogenic material into combined ash and shell midden layers. The shell in MF 5.3 is less fragmented than

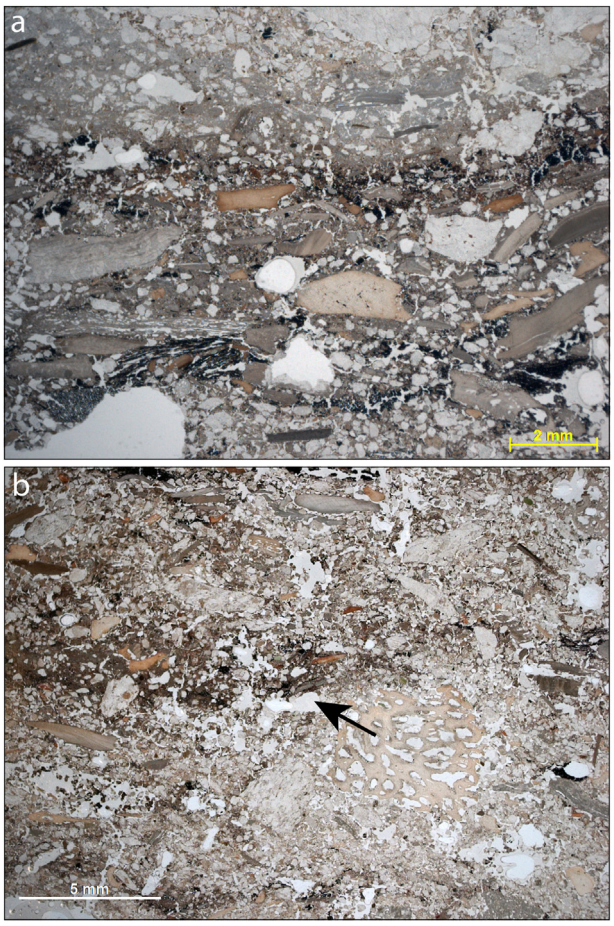

Figure 20. Stacked and single combustion features (both in plane-polarized light). a) Two hearths stacked directly one above the other in DCCP12. Note the thicker and more pronounced layers of carbonized organic material than those observed in the stacked hearths in Figure 18 (DCCP9). b) A single combustion feature at the base of DCCP11 within sediments of microfacies 1.2.1 The feature is probably the edge of a hearth but has been impacted by trampling.

in MF 5.2, but the visible in situ breakage and the mixing of material suggests some impact by trampling (Villagran, 2019). The secondary apatite which altered some of the ash in both MFs is biogenic in origin.

Calcite The extremely thin layer of mostly micritic calcite (MF 6.1) near the top of RSYS1 was formed through the precipitation of calcite from calcium-enriched water. Its clearly defined upper and lower boundaries and conformity to the underlying sediment suggest it was a thin crust, which formed on a stable surface, but its lateral extent beyond the slide is unknown as it is not visible to the naked eye in the profile. Speleothem and other forms of geogenic calcite are fairly common in other areas of KRM due to the dissolution of the calcite cement in the Geelhoutboom aeolianite by rainwater and the percolation of the resulting calcium-enriched water down through the quartzite host rock and into the various recesses that make up the complex (Butzer, 1982; Deacon and Geleijnse, 1988). The absence of clastic inclusions suggests that there was no clastic deposition in this location while the crust formed. The distinct accommodated planar void in areas where the calcite is no longer present (Fig. 15) indicates that the partial dissolution of the crust took place after the deposition of at least some overlying sediment. Therefore, it likely involved the movement of relatively acidic water through the deposit, perhaps as a result of guano breakdown.

4.2. Site formation in Cave 1B

The formation of each of the units/unit groups analyzed using micromorphology and μXRF is discussed in the following sections to explore general patterns in site-formation processes, including human behaviors, through time. Where appropriate, the micromorphology data are used to help interpret the macroscopic properties of deposits in the RS and DC, which were not included in the samples. The context of KRM 41815 is also considered.

The Middle Stone Age I in the RS deposits Due to the lack of microscale data, the formation of only a few of the most significant units in the unsampled portion of the RS is discussed here (see Fig. 21 and Table 3). The lowermost excavated unit in PP38, RSBR, is correlated with Layer 13a, which has previously been suggested to be the product of weathering during a hiatus (Singer and Wymer, 1982; Deacon and Geleijnse, 1988) and perhaps even a soil (Singer and Wymer, 1982:25). Surface stability in open-air archaeological contexts is typically associated with the pedogenic alteration of sediments resulting in the formation of soil horizons (Holliday et al., 2017). However, these horizons are very uncommon in caves and rockshelters, but a variety of diagenetic processes can weather deposits to different degrees during periods of surface exposure (Goldberg and Sherwood, 2006; Mallol and Mentzer, 2017; Mallol and Goldberg, 2017). The current exposure of RSBR is very limited, and the underlying deposit is not visible, but its macroscopic properties suggest greater diagenesis than in the sampled deposits. It does appear to represent a period of surface stability, but it cannot be considered a soil. The unit RSBCH (correlated with Layer 10) contains a relatively large proportion of anthropogenic materials, including dark lenses, which could be intact portions of charred deposits, in a relatively fine matrix (silty sand with some clay). This suggests that it could be the remains of a poorly preserved CP-like set of deposits. The clast-rich but artifact-poor RSDRU and RSYRU could reflect a period of relatively slow deposition or the winnowing of the deposit by water. The particularly clay-rich unit RSGBS2B could represent a period of surface exposure and weathering when the breakdown of material due to diagenetic processes increased the proportion of clay relative to other units (Farrand, 2001:555). The macroscopic properties of RSCP2 suggest it could be similar to RSCP1 (see below) but that the combustion features have been more heavily impacted by reworking and diagenesis.

The deposits in unit RSYBS, the lowest unit sampled for micromorphology (Fig. 4), are all primarily the product of geogenic deposition of shelly sand and quartzite (Fig. 9), but the inclusion of varying proportions of reworked ash and charcoal show that humans occupied Cave 1B during these periods and made fires within the shelter. The overlying RSCP1 is made up of several relatively poorly preserved in situ combustion features that have undergone mechanical reworking and minor chemical alteration. The properties of the MF 1.2.1 deposits in RSCP1T and the base of RSYS1 indicate a return to largely geogenic deposition with significant input of material from reworked combustion features. The rest of RSYS1 is overwhelmingly geogenic in character, with some biogenic inputs.

Macroscopically, there are some isolated artifacts and carbon-rich lenses (Table 3), but it appears that human occupation of Cave 1B was very limited at this time or took place in an entirely different area of the shelter with limited lateral reworking of anthropogenic material. The high density of autogenic quartzite (both sand- and gravel-sized) in the unit suggests a reduction in allogenic sedimentation, or more rapid breakdown of the host rock. However, the notable reduction in sand-sized shell fragments could be the result of partial dissolution of calcite in these deposits (e.g.,

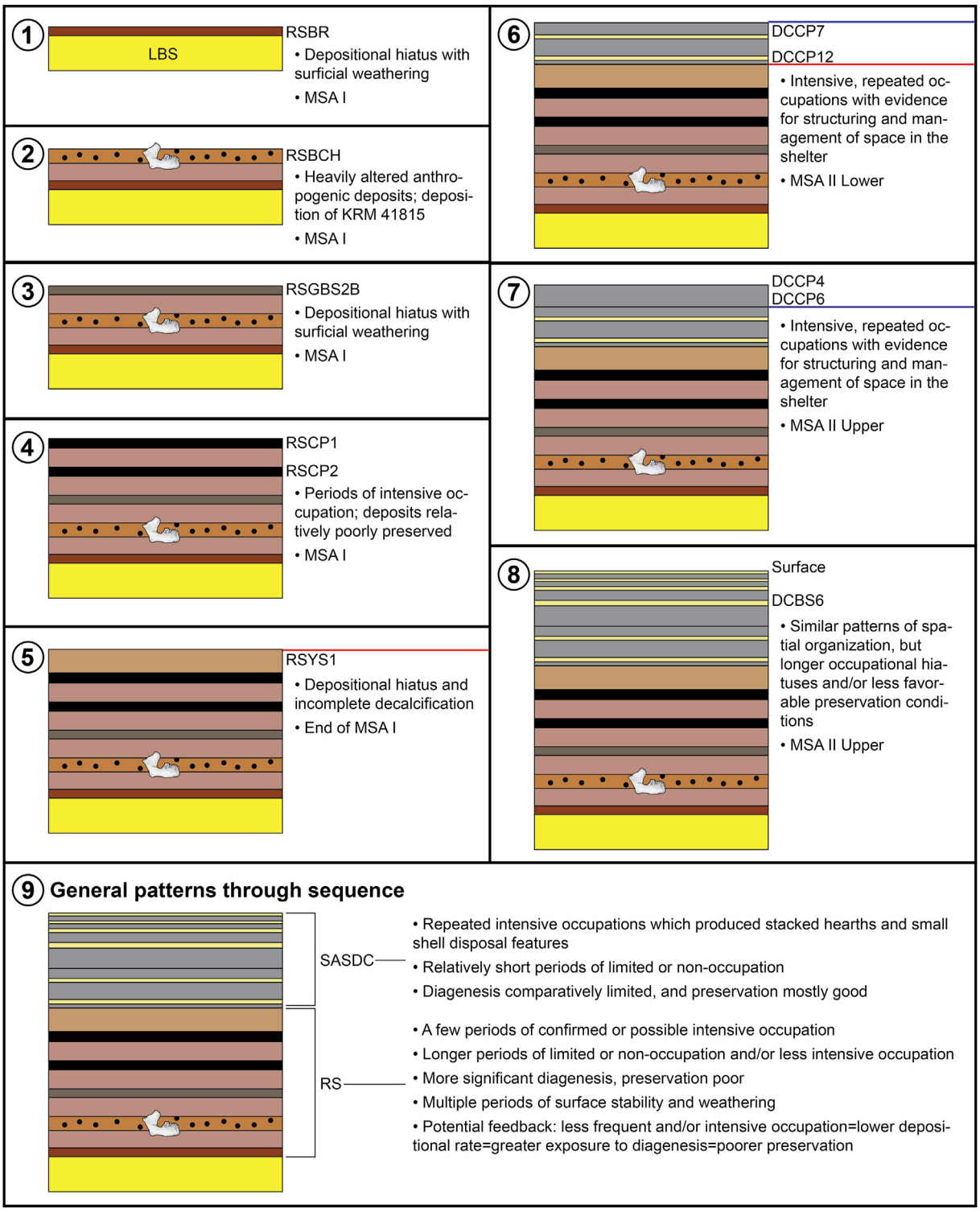

Figure 21. A simplified view (not to scale) of the proposed sequence of events in Cave 1B following the deposition of the Light Brown Sand (Panel 1), up to the deposition of the youngest preserved deposits (Panel 8). Only the most significant and/or informative deposits in the Rubble Sand Member are mentioned explicitly, but note the accumulation of other deposits between them. Panel 9 is a summary of the general patterns of anthropogenic site formation and diagenesis.

Goldberg, 2000), which would likely have removed any ash the deposits may have contained.

There were several short depositional hiatuses toward the end of RSYS1's formation. The thin calcite crust, overlying thin layer of quartzite and bone, and the incipient crust composed of secondary apatite nodules (Fig. 15) all indicate periods of surface stability in which clastic deposition ceased or slowed significantly for unknown periods of time. The resumption of deposition above the nodule layer corresponds with the transition to the MSA II–bearing DC deposits. These periods of surface stability could also be a factor

in the dissolution of shell fragments in the shelly sand and in the partial dissolution of the calcite crust. A time-gap between the deposits associated with the MSA I and II has previously been proposed across the site complex based on different unconformities or disconformities (Singer and Wymer, 1982; Deacon and Geleijnse, 1988).

The Middle Stone Age II in the DC deposits The micromorphology supports the macroscopic observation that the transition to the DC coincides with a marked increase in the preservation of anthropogenic deposits and features (Fig. 21). However, the preservation of any particular deposit can vary widely through the sampled sequence.

The basal unit group, DCCP12 (Fig. 4), is made up of two distinct phases (Fig. 10). The lower comprises deposits of MFs 1.2.1, 1.2.2, and 2.1, which are predominantly geogenic in nature but contain a relatively high proportion of reworked ash, charred organic material, and shell. This is likely due to lateral reworking of combustion features by trampling and indicates a resumption of more frequent and/or longer duration human occupation after the limited evidence for occupation in RSYS1. The upper portion of this unit group comprises alternating deposits of MFs 4.1 and 3.2, which are the remains of two hearths that appear to have undergone some reworking but are largely in situ. The ash-rich layers are very thin, and the lower of the two contains a relatively high density of shell and bone fragments. This suggests that there was either deliberate discard of shell and bone into the hearth or that distinct shell and ash layers have become mixed. The thinness of the ash could reflect reworking of some ash, compression due to trampling and the weight of overlying sediment, or even that the hearths each represent a single fire event and not multiple refirings (Karkanas 2021). The clear in situ fragmentation of roughly horizontal shell and bone (Fig. 16) is strongly indicative of trampling (Balbo et al., 2010; Villagran et al., 2011; Villagran, 2019), and this is interpreted as a trampled surface.

DCYS6 is strongly geogenic in character, mostly comprising shelly sand and quartzite. However, the presence of ash and charred organic material, the size of some of the shells in the unit, and a very thin ash lens all point to at least some human occupation which included making fires.

The DCCP11 unit group is characterized by a generally geogenic, but ash-rich, sediment with several distinct deposits of more concentrated anthropogenic material which thin out and end within the slide (Fig. 10). The ash at its base, which includes sand and bone fragments, could represent the edge of a hearth that has been reworked by trampling. The thin layer rich in carbonized material (MF 4.1) has no distinct ash layer over it, suggesting this material was removed by geogenic or anthropogenic processes. The most significant deposit is a wedge of ashy shell-dominated sediment (MF 5.1). This appears to represent the edge of a small, locally reworked shell disposal feature. As trampling is more likely at the edge of such a deposit, this could well be responsible for the shell fragmentation and the mixing of ash and sand into this feature, but it is also possible that some ash was deliberately discarded with the shell. The presence of two thin winnowed deposits (MF 2.1) above this feature suggest some localized water movement at the surface after its formation.

DCYS5 is absent from the thin sections, but comparing its field description to those of sampled deposits (Table 3) suggests that it is predominantly geogenic but with a significant component of ash and charred organic material from reworked combustion features, broadly comparable to MF 1.2.1. DCCP10 is also not represented in the thin sections, but a similar composition suggests it is probably similar to DCCP11 in containing layers of ash- and organic-rich sands similar to particularly silty MF 1.2.1 deposits and ashy deposits broadly similar to MF 3.2 (and perhaps 3.1).

Only a very small portion of DCYS4 appears in the thin sections (Fig. 11). This deposit is sandy but very rich in charred organic material and ash. As with many deposits of this type, it is very likely the product of the reworking of material from combustion features into otherwise largely geogenic sediment. The deformed apatite-rich lens at the top of this unit, seemingly an incipient crust, indicates a period of surface stability, followed by deformation of the sediment due to trampling.

DCCP9 is the thickest of the CP unit groups represented in the thin sections. The first few deposits are sloping layers of shell-rich ash with rounded quartzite pebbles (MF 5.3). It is possible that they are the product of the mixing of originally more distinct shell and ash deposits, or the reworking of a combined ash and shell midden. The size of the shell fragments, and evidence for in situ fragmentation, suggest trampling likely played a role in this mixing (Villagran, 2019). These deposits are overlain by two well-preserved hearths (MF 3.1), which include extremely thin layers of phosphatized ash, and lenses of sand, indicating that each of the hearths likely formed through multiple burning events. Apart from some alteration by secondary calcite and apatite, and very limited bioturbation by soil mesofauna, these deposits have seen little modification or disturbance. It is possible that at least some of the sand in the less preserved hearths in the sequence was originally in the form of similar lenses prior to mixing into the surrounding ash by trampling. The upper surface of this group of hearths represents a disconformity, which is locally unconformable. The ash at the surface is relatively highly phosphatized, in a band notably thicker than the laminae below, indicating a longer period of surface exposure, while depressions suggest localized erosion of ash. This unconformity/disconformity is overlain by a very ashy sand (MF 1.2.1) with some ash-dominated patches, which is capped by a thin ash lens. It seems to be the product of the reworking and mixing of anthropogenic and geogenic deposits. The overlying shelly and carbon-rich deposit (MF 5.1) appears to be the base of a hearth where the substrate included shells. The in situ fragmentation of the shells and their roughly horizontal orientation indicates trampling (Villagran, 2019), and this appears to represent a trampled surface. The preservation of relatively large charcoal fragments could indicate that burning took place following the trampling. The ash deposits above include some relatively large pieces of possibly burnt bone and shell and fairly big pieces of quartzite, some of which could be lithics. Alternating MSUs of more and less charred organic-rich ash suggest that these deposits may represent several hearths stacked on one another which were subsequently modified through the mixing of sand into the ash and resulting loss of stratigraphic detail. The overlying ash deposits contain significantly more quartzite and are obviously more geogenic in character than those below. Some pockets are similar to MF 1.2.1, suggesting far more significant reworking and mixing than in the hearths below. The in situ fragmentation of some shell near the top of this sequence could be the product of trampling. The uppermost deposit is a sandy deposit (MF 1.2.1) with some ash, charred material and shell that is predominantly geogenic, and transitional to the unit mentioned earlier.

DCYS3 is initially very strongly geogenic in nature, with some biogenic inputs, and has a similar density of autogenic quartzite to RSYS1 (MF 1.1). However, there is an increasing anthropogenic signature towards the top of this thin unit as ash and charred organic material fill some of the interstitial space between the sand and gravel (MF 1.2.1). This points to a period with no or extremely limited human occupation, followed by human occupation and reworking of combustion features. As with RSYS1, however, the

limited proportion of sand-sized shell in the lower part of DCYS3 could be due to post-depositional dissolution of calcite, which would also impact any ash that may have been in this deposit.

The basal MSU in the overlying DCCP8 unit group shows a lateral transition from potentially in situ, but locally reworked, ash to a sandier deposit with reworked ash and charred organic materials. This is very likely the edge of a combustion feature, where trampling and other human activities have dispersed and mixed these materials (e.g., Miller et al., 2013). This is followed by a very well-preserved hearth (MF 4.1, 3.1, and 3.2), which appears to have been formed by multiple fires based on the presence of distinct extremely thin lenses of sand and of phosphatized ash. The shell at the base of this hearth was trampled prior to the burning and represents a trampled surface, while some of the shell at the top of the hearth may have been pressed downward into the ash by trampling. Overlying this hearth is a succession of distinguishable, but less well-preserved hearths, with alternating charred material-rich (MF 4.1) and ash deposits (MF 3.2). The ash in the uppermost few hearths is relatively highly phosphatized, and there appears to have been an erosional event that truncated the top hearth. This suggests a hiatus with the ash being exposed on the surface for some time. The deposit lying on this sloping truncated surface is a mix of geogenic and anthropogenic materials, which includes a high proportion of relatively large quartzite (some of which are lithics; MF 2.2). It is possible that this represents localized colluvial deposition of mixed material, filling the cut below. The uppermost MSU in DCCP8 that is represented in the thin sections is an ash-dominated but mixed deposit, suggesting reworking of a combustion feature. Shell fragmentation and the apparent pressing of a shell into the sediment are indicative of trampling.

None of the deposits above DCCP8 have been sampled, but it is possible to make some broad interpretations based on the micromorphology and the macroscopic properties of the sampled and unsampled portions of the DC. The deposits appear fairly similar up to the top of DCCP4, but from the base of DCBS6 there is a shift towards thinner CP unit groups separated by thicker sandy units, which appear to contain a lower concentration of fine organic material and ash than most of the sandy units below. This could be due to longer occupational hiatuses, greater exposure of the shelter leading to less preservation of fine anthropogenic materials, more rapid deposition of sand, or a combination of these factors. The sandy unit excavated by Henderson (1990) in the squares to the west of PP38 contained a fairly high density of lithic artifacts and bone but no distinguishable combustion features or shell concentrations. This suggests that the sandy units through the sequence cannot automatically be assumed to represent hiatuses, but many could reflect limited preservation of anthropogenic features, rather than nonoccupation.

The CP and PCP units in the area excavation contained numerous anthropogenic features, including stacked hearths and small shell disposal features (Henderson 1990, 1992). The spatial organization of these features had a significant impact on the sedimentary properties of the deposits, concentrating ash, charred organic material, and shell in particular areas of the excavation. This is particularly evident in DCPCP, where numerous combustion features were concentrated in one area, and the surrounding sediment gradually lightens from black to brown, presumably due to a decrease in the quantity of charred organic material in the sediment further away from the combustion features. The concentration of combustion features and the presence of the small shell disposal features have both been interpreted as evidence for the organization of space within the shelter by the occupants, while the burnt shell is attributed to the cooking of shellfish (Henderson, 1992).

The sedimentary properties reported by Henderson (1990, 1992) suggest broadly similar formation processes for the uppermost CPs in the preserved sequence to those inferred for the CPs lower down in the DC. The spatial variation within the CPs is similar to those described in PP38 (Table 3), although the lateral variation in DCPCP appears to have been more extreme than was observed for any of the CPs in PP38.

Formation and preservation of anthropogenic features The "carbonaceous soil" reported in various layers of the original excavation by Singer and Wymer (1982:24–25) appears to be broadly comparable to the CPs defined by the Deacon team. The formation of the "carbonaceous soil" was never explicitly addressed by Singer and Wymer (1982). The bulk of the sediment in the CPs at KRM—dark silty sands around the distinct combustion features—has been argued to be the product of the burning of the inedible portions of plants, including geophytes, during food processing and cooking (Deacon, 1993, 1995). Direct evidence for the consumption of cooked geophytes at Klasies has been recovered from MSA I and HP deposits, suggesting a long history of this behavior at the site (Larbey et al., 2019).

Our micro-scale observations of the CP units indicate that lateral reworking of combustion features has resulted in the formation of deposits characterized by variably preserved combustion features (including hearths), and less common small shell disposal features, surrounded by sandier deposits rich in reworked ash, carbonized material, and other anthropogenic inclusions. This is most clearly visible in the thin sections in DCCP11 (Fig. 10) and at the base of DCCP8 (Fig. 11). These deposits represent repeated relatively intensive occupations of the shelter.

Trampling played an important role in reworking material around hearths to form the CPs. Evidence of trampling as a site formation process has been identified at almost every MSA cave or shelter site studied with micromorphology in South Africa, although its importance varies (Goldberg, 2000; Goldberg et al., 2009; Karkanas and Goldberg, 2010; Miller et al., 2013; Karkanas et al., 2015; Wadley et al., 2020; Haaland et al., 2021; Wurz et al., 2022). In contrast, the identification of trampled surfaces (e.g., Figs. 16 and 17) is far less common in the region, with previous published examples from only Sibudu Cave (Goldberg et al., 2009) and Diepkloof Rock Shelter (Miller et al., 2013). Most of the trampled surfaces in Cave 1B are characterized by in situ fragmentation of horizontally oriented shell, with some indication of compaction (Fig. 16). Similar trampling has been identified in Cave 1 (Wurz et al., 2022: fig. 5). These surfaces are most comparable to well-studied occurrences of trampling in shelly deposits at coastal sites in South America, which have broadly similar substrates to KRM (Balbo et al., 2010; Villagran et al., 2011; Villagran, 2019).

Anthropogenic deposits are uncommon in the RS (Fig. 6). Only two CPs were identified by the Deacon team, and smaller deposits of ash or charred material are rare (Table 3). The CPs in the RS are almost exclusively composed of dark silty sands rich in charred organic materials, with few or no macroscopically distinguishable ash deposits. Darker deposits lower down in the sequence could be poorly preserved occupational deposits (Singer and Wymer, 1982), with RSBR the most convincing example. Small shell disposal features are absent in the RS samples, and the limited presence of visible shell in the unsampled deposits (Table 3) also stand in contrast to the properties of the DC.

Shell midden deposits and distinct combustion features have been recorded in MSA I deposits in Cave 1 and 1A (Singer and Wymer 1982; Deacon and Geleijnse, 1988; Wurz et al., 2022). This raises the question of whether the pattern observed in the RS is a result of behavioral differences between these areas (e.g., Cave 1B being used for different activities, less frequently, or less intensively) or the product of diagenetic processes.

The association of parts of the MSA I with one or both MIS 5e sea-level highstands suggests that Cave 1B could have been more exposed to onshore winds at this time. In comparison, sea-level regression after the peak of MIS 5e (~120 ka) could have resulted in the formation of barrier dunes during the MSA II, which would have provided some protection for the site, as argued by Deacon (1995). Greater exposure to wind during the MSA I could have contributed to the destruction or alteration of deposits by eroding ash and fine burnt material from exposed combustion features and by blowing more rain into the shelter than would otherwise enter this area. Additionally, closer proximity of the shoreline to the site could increase the impacts of sea spray and the potential for the erosion of the outer areas of the shelter by storm waves. These factors could also have decreased the attractiveness of Cave 1B for occupation during the MSA I.

It is also possible that the unsampled RS deposits were more heavily impacted by the dissolution of guano—and resulting increase in the acidity of pore water—than the sampled units. This process can result in varying degrees of alteration or destruction of ash, shell, and bone depending on local conditions (e.g., Schiegl et al., 1996; Goldberg 2000; Weiner et al., 2002). There is evidence to suggest that these diagenetic processes have destroyed significant midden deposits and combustion features in areas of Cave 2 (Wurz et al., 2022). Surface stability during the observed hiatuses in the RS sequence would have increased the likelihood and impact of this process.

Anthropogenic depositional rates are higher than geogenic rates, but also more sporadic, so more intensive and/or frequent anthropogenic depositional events result in shorter exposure times for most deposits. As the observed diagenesis in Cave 1B all occurred at or near the surface, there would have been feedback between anthropogenic depositional rates (and thus, the nature of human occupation) and the likelihood of anthropogenic deposits being preserved well, or at all (Fig. 21). Therefore, it is very likely that the pattern observed in the RS is due to both greater diagenesis than observed in the DC, and comparatively limited and/or less intensive human occupation during the MSA I.

In stark contrast to the RS, anthropogenic features are numerous and well preserved in the DC deposits, making up a significant proportion of its thickness. Hearths are very common within the CPs, and most are stacked.

The presence of phosphatized surfaces and sand and quartzite lenses of varying thicknesses within stacked sequences or between groups of hearths within a single CP suggest that some CPs may have formed over the course of several distinct occupations with relatively short hiatuses between them (perhaps seasonal or even monthly visits). Stacked hearths representing multiple firings in a short period of time have previously been reported from the MSA I occupations in Cave 1 and the HP deposits in Cave 1A (Larbey et al., 2019).

The shell-rich MFs 5.2 and 5.3 share some similarities in composition and structure with reworked midden deposits across the rest of the site complex (Wurz et al., 2022). As these deposits in Cave 1B have extremely limited spatial extent and low thickness relative to their degree of compression when compared to the MSA I and II middens in Cave 1 and 1A, it is more appropriate to continue to describe them as shell disposal features, as suggested by Henderson (1992), rather than middens. However, the micromorphology suggests they are functionally the same thing—a specific place to discard shell (and perhaps also ash). The major difference is the size and thickness of the original feature and thus the intensity and/or frequency of their use for this function. Unfortunately, it is difficult to assess whether this is due to relatively limited consumption of shellfish in Cave 1B in comparison to the rest of KRM, the existence of an unidentified (or even destroyed) midden elsewhere in or near the shelter, or other behavioral and/or preservation factors.

The presence of stacked hearths and shell disposal features are both indicative of the organization of domestic space within the shelter during human occupations of Cave 1B. The behaviors involved in organizing and managing space in Stone Age contexts are among the multiple proxies used by archaeologists to understand the evolution of modern human cultural practices and cognitive abilities (Clark et al., 2022). Various expressions of such behaviors have been documented throughout the MSA and Middle Paleolithic (e.g., Deacon, 1995; Roebroeks and Villa, 2011; Wadley et al., 2011, 2020), with a general intensification of the organization and management of occupation sites and changes in the use of domestic spaces (Clark et al., 2022).

The stacked hearths and shell disposal features identified by Henderson (1992) in the upper portions of the MSA II indicate organization of space in the shelter late in this cultural phase, but our results show that this behavior took place in Cave 1B throughout the MSA II, almost certainly from before ~110 ka (based on the new dating of basal SAS deposits by Wurz et al., 2022).

Implications for the context of KRM 41815 The KRM 41815 mandible and the associated KRM 41820 condylar fragment were found next to the calcite block in Wymer's western profile (Singer and Wymer 1982:146). Their close proximity to the northern profile of PP38 (Fig. 1) means that the properties of RSBCH (Table 3) are likely very similar (or even identical) to the context from which they were recovered. As the conditions in Cave 1B are not conducive to the formation of speleothem, the calcite block almost certainly formed outside of the shelter. It is very likely a large piece of the tufa/phytokarren, which formed on the host rock above the complex.

The properties of RSBCH are suggestive of very poorly preserved occupation deposits, which may once have been similar to the CPs in the overlying deposits. The micromorphology of the CPs in the upper RS and in the DC points to both physical reworking and chemical diagenesis as factors influencing the preservation of anthropogenic deposits.

It is tempting to attribute the breakage of KRM 41815 to the impact of the block falling into the site, and the resulting deformation of deposits, but this event could predate the deposition of the specimen. Trampling and the accumulation of overlying deposits could also be responsible for the damage. Wind and water movement may also have contributed to physical reworking of finer materials within RSBCH.

The mandible has been described as “well-mineralized” (Singer and Wymer, 1982:146). Calcite appears to be the most likely mineral in this case, but no further information is available to confirm this. Observations from the sampled deposits suggest it is very likely that RSBCH has been impacted by the precipitation of secondary minerals (including calcite and apatite) and the dissolution of primary calcite.

Although KRM 41815 was not recovered from a well-preserved group of deposits, it was likely in either primary or near-primary (very limited movement from point of deposition) context. However, the impact of post-depositional processes has implications for correlating this deposit (and over- and underlying deposits) with units elsewhere in the site complex (which is already a difficult task for well-preserved anthropogenic units). Sampling and microanalysis of RSBCH and adjacent deposits would provide stronger evidence on which to evaluate the specific context and assess the accuracy of our inferences.

4.3. Stratigraphy

Deacon's excavation units in PP38 are far more constrained than Wymer's layers, typically representing single macroscopically distinguishable deposits, except where deposits are so thin or localized that it was not practical to excavate them separately (e.g., some dark charred layers underneath ash deposits). However, these excavation units were found to contain multiple MSUs (Figs. 9–11). DCCP11, which was excavated as a single unit, contains nine MSUs, and DCCP9, which comprises six grouped excavation units, was found to be made up of 20 MSUs. This information is important for interpreting material excavated from PP38 because, despite the high-resolution excavation approach, the assemblages recovered from the units cannot be considered the product of a single event, although the events forming some units may have taken place within a relatively short period of time.

Given the difference in resolution of excavation and recording and the limited descriptions provided by Wymer, it would never be possible to correlate the Wymer and Deacon stratigraphy with total precision, even without the lateral variation observed at multiple scales in many deposits in Cave 1B. However, the new correlations suggest that the transition between the RS and DC in PP38, and thus the MSA I and MSA II lower cultural phases, corresponds to the contact between Wymer's Layers 5 and 4, while the shift from the MSA II lower to the MSA II upper falls within Layer 3 (Table 4). This contrasts with Hilary Deacon's correlations between Wymer's layers and the PP38 units (published in Wurz, 2002), which placed these cultural changes at the boundaries between Layers 12 and 11 (MSA I to MSA II lower), and Layers 6 and 5 (MSA II lower to MSA II upper) respectively (Table 2). However, the labeling in the previously unpublished Figure 5 (from the Deacon archive) is in agreement with our correlation of Layer 10 with RSBCH. As no details of the data or reasoning used by Deacon are published (and none have been found among available unpublished materials), it is impossible to discuss why they differ so greatly from the revised correlations or the earlier assessment in the previously unpublished Figure 5 without resorting to conjecture. The implications of these new data for stratigraphic correlation with the rest of the complex and the age of the KRM 41815 mandible are discussed in the following sections.

Correlation with the rest of the complex Lithostratigraphic systems such as the one in use at KRM (Fig. 2) are based on the grouping or division of deposits based on their visual properties—including the color and composition of sediments. As a result, post-depositional alteration of deposits by chemical and physical processes (which likely varied spatially across the complex) is a significant complicating factor for making lithostratigraphic correlations. This is of particular concern for understanding how the mostly unsampled RS deposits relate to the MSA I deposits in Caves 1 and 1A.

Due to the rare use of the names RS and DC for the deposits in Cave 1B, the very limited and conflicting published information available on this part of the complex and the fact that the RS deposits are associated with MSA I lithics, it is easy to conflate the RS with the LBS (e.g., Morrissey et al., 2022). Given the culture-stratigraphic nature of the SAS Member (Morrissey et al., 2022), and the presence of MSA I lithic technology throughout the RS deposits (Wurz, 2002), it is clear that the RS cannot be included in the SAS as a submember as suggested by Deacon and Geleijnse (1988), Deacon and Schuurman (1992), and Henderson (1992) prior to the exclusive association of the SAS with the MSA II.

The RS is broadly similar to the LBS across KRM in that the nonanthropogenic deposits are predominantly yellowish brown or light brown sands (Deacon and Geleijnse, 1988:8). However, there are also notable differences based on published descriptions (Deacon and Geleijnse, 1988) and field observations of the LBS, and the RS and LBS in PP38 were considered to be distinct entities (Fig. 5). The lower RS deposits contain more silt and clay, and there are no published examples from the LBS of deposits such as the extremely clast-rich deposits at the top of the RS. Likewise, none of the deposits are similar enough to the 'RBS' to suggest a lithostratigraphic correlation with this entity as defined by Deacon and Geleijnse (1988:9). The fact that Deacon and Geleijnse (1988:11) recognized a change in sedimentary properties from the LBS to the RS does not mean this automatically correlates with the transition from the LBS to the 'RBS' in Cave 1, especially because the difference in properties could be due to post-depositional processes rather than a change in depositional processes.

Based on a review of past studies, Morrissey et al. (2022) raised the question of whether the RS should be included in the LBS as a submember, considered a member in its own right, or even placed into a more broadly (re)defined LBS. Due to our new observations of the differences in lithology, we argue that the RS deposits should not be grouped in with the LBS, the 'RBS', or the SAS and should instead be classified as the RS Member, a distinct stratigraphic entity associated with the MSA I (Fig. 2). Due to the differing contexts of Caves 1, 1A, and 1B, and the lack of dating, the RS Member's correlation with the LBS and 'RBS' members is uncertain.

The alternating deposits of sand and dense anthropogenic units preserved in the DC are broadly similar to the SAS Member in Cave 1A (Deacon and Geleijnse, 1988). However, they differ from the four SAS submembers in the Cave 1 Witness Baulk (Fig. 2), being sandier and more clearly stratified than the SASL and SASU, and in primary or near-primary context unlike the talus deposits in the SASW and SASR (Deacon and Geleijnse, 1988; Wurz et al., 2018).

The significant lithological diversity of the deposits assigned to the SAS means that it is more useful to consider it a cultural grouping of the MSA II–bearing deposits below the RF Member (Fig. 2) rather than a lithostratigraphic member similar to the more uniform LBS (Morrissey et al., 2022). Therefore, the best option appears to be to follow Henderson (1992:17) and retain the DC deposits within the SAS as a submember. Following the established naming convention but also retaining the full abbreviation to avoid confusion, the submember is designated as the SASDC (Fig. 2).

The SASDC presents a challenge from a lithostratigraphic perspective. The deposits are clearly distinguishable from the underlying RS Member due to the presence of dense accumulations of anthropogenic materials and features. However, there are notable similarities in the properties of the predominantly geogenic units in the upper RS and the SASDC. Distinguishing this boundary could be significantly more difficult in currently unexcavated areas of Cave 1B. Given the nature of the CPs, the properties of the RS and SASDC would only be consistent across the shelter if the same behaviors were happening (or not happening) across the extent of the site throughout the periods of occupation, which is unlikely. This is an inherent problem with the use of anthropogenic deposits as defining characteristics of lithostratigraphic groupings. Spatial variation in preservation could also have a significant impact, such as that observed in Cave 2 (Wurz et al., 2022). It is possible that the SASDC has been heavily impacted by dissolution and phosphatization elsewhere in the shelter or that the MSA I occupations are better preserved in other areas. If the distinct pattern in PP38 were not present in other excavations, the use of lithic techno–typological analysis to determine cultural stratigraphy would become even more important.

Implications for the age of KRM 41815 Being able to confidently associate KRM 41815 with the MSA I is an important step given that it has variously been assigned to the MSA I and the MSA II in different publications for several decades (e.g., Deacon and Geleijnse, 1988; Deacon, 2008; Grine et al., 2017b, 2021, 2023).

Whenever the mandible has been assigned to the MSA I previously, it has been considered contemporaneous with Layer 37/the 'RBS' Member. This is due in large part to the relative dating conducted by Goede and Hitchman (1987), which suggested a similar age for Layer 10 and Layer 37. They noted significant potential for variation in uranium enrichment, which could skew the ages of samples, but did not attempt to make corrections for this variation. Given the potential for differences in depositional and post-depositional processes between Cave 1 and Cave 1B, this correlation is particularly likely to have been affected by this problem.

As Layer 10 is relatively deep within the RS and the only evidence for a direct correlation with the 'RBS' is not ironclad, the possibility that it could correlate with part of the LBS in Caves 1 and 1A rather than the 'RBS' must be considered. It must also be noted that because depositional rates in different areas of the site are not well understood, and truncation of the LBS has been reported in parts of the site (Deacon and Geleijnse, 1988), depth cannot be assumed to be a reliable indicator of relative age. The fact that the LBS, 'RBS', and RS are all MSA I–bearing (Wurz 2002) further complicates correlation.

KRM 41815 (and the missing KRM 41820) is very broadly contemporaneous with six confirmed human fossil specimens which have also been associated with the MSA I (Grine et al., 2017b). KRM 24396 (SAM-AP 6297) was excavated from Layer 38 in Cave 1 but was not analyzed by Singer and Wymer (1982). It was subsequently identified as a cranial vault fragment, perhaps parietal or supraoccipital (Grine et al., 2017b). It is the only confirmed human specimen from 27 cranial vault pieces from Layer 38, which could not be located by Ronald Singer when he analyzed the human fossil assemblage (Singer and Wymer, 1982: table 8.1; Grine et al., 2017b). Hilary Deacon subsequently recovered two maxillary fragments from shell midden deposits in the LBS Member at the Cave 1/1A boundary (Rightmire and Deacon, 1991). Measurements of these fragments revealed a greater similarity to Holocene-comparative specimens than to a sample of archaic or early modern *H. sapiens* specimens (Bräuer et al., 1992). The size difference between the two maxillae has also been interpreted as evidence for sexual dimorphism (Rightmire and Deacon, 1991). The excavation of Layer 37 in Cave 1 yielded three cranial vault fragments: KRM 26909 (SAM-AP 6105), KRM 26910, and KRM 27070 (SAM-AP 6106) (Singer and Wymer, 1982). The first specimen is most likely a parietal fragment, the second was never analyzed, and the third is also considered to be a parietal (Singer and Wymer, 1982; Grine et al., 2017b).

The MSA I has been dated using several different absolute and relative dating techniques, but the results require careful interpretation. Samples from speleothem associated with the base and top of the LBS in Cave 1, but not directly associated with archaeological deposit at the time of sampling, were dated using uranium thorium (U–Th) but yielded contradictory ages, with the results suggesting that the LBS is older than 110 ka in one case (Deacon et al., 1988) but younger than ~109 ka in the other (Vogel, 2001). These dates were reported with extremely limited contextual information (none in the case of Deacon et al., 1988), making it practically impossible to independently assess how they relate to the LBS deposits or to each other (see also Wurz et al., 2022). Vogel (2001) did not discuss the discrepancy or even mention the previous publication of a U–Th date. This is particularly problematic, given that the two results are in direct opposition.

A sediment sample collected from roughly halfway up the LBS Member deposits at the Cave 1/1A boundary yielded a result ranging widely from ~119 ka to ~94 ka based on a combination of thermoluminescence and optically stimulated luminescence dating (Feathers 2002). Feathers (2002:178) noted significant challenges for estimating radioactive dose rates, which are vital for interpreting luminescence results to produce age estimates. He also suggested that the true age of the sample was more likely to fall within the older end of the range produced (Feathers, 2002:191).

Aspartic acid racemization (AAR) dating of bone from Layers 37 and 38 in Cave 1 produced ages of 90 ka and 110 ka, respectively (Bada and Deems, 1975). These ages were estimated using a calibration developed by AAR-dating a bone from ^{14}C-dated Terminal Pleistocene deposits at Nelson Bay Cave, roughly ~90 km west of KRM. It was assumed that the similar climate would mean that bone at both sites would have been exposed to similar temperatures and would thus have experienced the same rate of racemization since their deposition. This is problematic, given that there was significant climatic variation between the start of the Late Pleistocene and the deposition of the bone used in the calibration at ~17 ka (Thackeray, 1992; Blome et al., 2012; Loftus et al., 2017; Reynard, 2021). Since the publication of these results, a number of challenges have been identified with the use of AAR dating of bone in archaeological contexts, particularly for older studies conducted with less sophisticated equipment or relying on ^{14}C calibrations produced prior to the introduction of accelerator mass spectrometry (Thackeray, 1992; Miller et al., 1999; Moini et al., 2013). There is even evidence to suggest that the species of animal is a factor in the rate of racemization of the bone (Moini et al., 2013). Concerns over the uncritical use of these dates at KRM were first raised by Anne Thackeray (1992:403), but there has been little other engagement with these issues.

The results of oxygen isotope analysis of shell from the LBS in Cave 1, the Cave 1/1A boundary, and the RS in Cave 1B were used to provide a relative age estimate based on the comparison of these values to the isotopic characteristics of dated marine cores (Shackleton, 1982; Deacon et al., 1988). They were argued to best match MIS 5e, suggesting an age range of between 130 ka and 115 ka for the shells. No data were provided for where within Wymer's layers 38 (Cave 1) and 12 (Cave 1B), the dated shell was collected, and only a single shell was dated per layer (Shackleton, 1982). Deacon et al. (1988) provided no data and no detail on the number of shells they dated or from where within the LBS they were recovered, but this information was eventually published by Thackeray (2018).

Recent results from U–Th dating of well-contextualized speleothems indicate that the basal MSA II–bearing deposits in the SAS in Cave 1 accumulated before 110 ka (Wurz et al., 2022). The speleothems were carefully sampled to date the oldest part of each and thus, provide the age at which speleothem formation began following the deposition of the basal unit in the SASL submember. This means that both the 'RBS' and LBS must predate 110 ka, and perhaps significantly so, given that the maximum age of the SASL is unknown. This is supported by a recent faunal study, which found that the environmental signal derived from the MSA I faunal assemblages points to conditions more akin to the MIS 6 glacial (188 ka to 130 ka) than the interglacial conditions associated with MIS 5e (Reynard and Wurz, 2020).

On the balance of evidence and considering the issues raised with the published absolute dates for the MSA I, KRM 41815 must predate 110 ka, and its age likely falls within early MIS 5e or MIS 6. KRM 41815 has the most developed chin of the mandibles recovered from KRM (Rightmire and Deacon, 1991). As the other specimens are from the MSA II, with ages perhaps as young as ~85 ka for some (Vogel, 2001), the unambiguous association of this specimen with the MSA I adds greater support to Grine et al.'s (2021:4) observation that "there seems to be a counterintuitive temporal trend for chin development" in the KRM assemblage. A clearer age for KRM 41815 would provide greater context to this pattern. Dating of well-contextualized U–Th samples is needed to clarify the age of the MSA I in the 'RBS' and LBS Members in Cave 1 and to

allow extrapolation of these dates to other areas of the complex, which lack in situ speleothem, including the RS Member. The lack of evidence for bioturbation suggests that luminescence dating could be an option for obtaining direct dates for the Cave 1B sequence, with due regard for potential challenges in estimating dose rates (see Feathers, 2002).

5. Conclusions

The multiscale data presented here provide greater insight into the stratigraphy and formation of the deposits in Cave 1B than previously published information allows. A range of anthropogenic, geogenic, and biogenic site-formation processes were identified in the PP38 sequence, with implications for understanding human behavior in Cave 1B and for making stratigraphic correlations with the rest of the Klasies complex. The stacked hearths in the well-preserved CPs within the SASDC show repeated use of the site over short periods of time, with clear spatial organization of activities. The small shell disposal features also reflect management of space. It appears that roughly the same degree of spatial organization and management was repeated during different periods of occupation for the duration of the MSA II/Mossel Bay cultural phase. Anthropogenic deposits are poorly preserved in the RS Member, due at least in part to the precipitation of secondary apatite. Multiple depositional hiatuses and resulting periods of surface stability and weathering likely contributed to this pattern. However, occupational frequency and/or intensity may also have been lower during the MSA I. Micromorphology sampling of more of the RS sequence would help to understand variation in site formation during the MSA I, would provide better context to KRM 41815, and could aid in identifying the impacts of post-depositional processes on the stratigraphy of the RS.

Several significant conclusions have been reached regarding the stratigraphy of PP38 and its relationships to the rest of the main site complex. The MSA I–bearing RS deposits correlate with Wymer's Layers 13a to 5, while the DC deposits, associated with the MSA II, are equivalent to Layers 4 to 1. The RS deposits should be considered a distinct lithological member and not a submember of the SAS or LBS Members. However, it is appropriate to retain the DC deposits as a submember of the SAS Member, designated as the SASDC. The cultural stratigraphic phases determined through lithic technotypologies remain the only means of making secure (but broad) temporal correlations between Cave 1B and the rest of the complex.

Finally, the revised stratigraphic correlations show that the KRM 41815/SAM-AP 6222 human mandible recovered from Wymer's Layer 10 is clearly associated with the MSA I cultural phase, and not the MSA II. However, it is not possible to definitively correlate Layer 10 with either the LBS or the 'RBS' in Cave 1, preventing a more secure determination of whether the mandible dates to an earlier or later phase of the MSA I. While this specimen definitely predates the ~110 ka speleothem within the SASL submember, the lower limit for its age is unclear, with the MSA I potentially extending back into MIS 6. Given that the mandible is among the most morphologically modern specimens recovered from Klasies, with a relatively strongly developed chin, being able to confidently associate it with the oldest cultural phase at the complex and a potential age of MIS 6/early MIS 5 is significant.

Acknowledgments

The authors wish to acknowledge the use of photographs and a profile drawing produced by the late Hilary Deacon and his excavation teams. Another of their profile drawings was redrawn digitally by Liezl van Pletzen-Vos. The support of GENUS (DSI-NRF Centre of Excellence in Palaeosciences, UID 86073 to P. Morrissey, and Grant 86073 to S. Wurz) toward this research is hereby acknowledged. The authors also wish to acknowledge the Palaeontological Scientific Trust (PAST) for a fieldwork grant and the Baden-Württemberg Ministerium für Wissenschaft, Forschung und Kunst for funding a research fellowship to P. Morrissey to facilitate the micromorphological analysis. Funding for the processing of the micromorphology samples was provided by a Baden-Württemberg Stiftung Elitepostdoc grant to S. Mentzer. Opinions expressed and conclusions arrived at are those of the authors and are not necessarily to be attributed to any of these funders. We thank three anonymous reviewers, Associate Editor Chris Campisano, and Co-Editor-in-Chief Andrea Taylor for comments which led to the improvement of this manuscript.

References

Bada, J.L., Deems, L., 1975. Accuracy of dates beyond the 14C dating limit using the aspartic acid racemisation reaction. Nature 255, 218–219.
Balbo, A.L., Madella, M., Vila, A., Estévez, J., 2010. Micromorphological perspectives on the stratigraphical excavation of shell middens: A first approximation from the ethnohistorical site tunel VII, tierra del fuego (Argentina). J. Archaeol. Sci. 37, 1252–1259.
Bergmann, I., Hublin, J.J., Gunz, P., Freidline, S.E., 2021. How did modern morphology evolve in the human mandible? The relationship between static allometry and mandibular variability in *Homo sapiens*. J. Hum. Evol. 157, 103026.
Binford, L., 1984. Faunal Remains at Klasies River Mouth. Academic Press, Orlando.
Binford, L.R., 1986a. Reply to: On Binford on Klasies River mouth: Response of the excavators. Curr. Anthropol. 27, 57–62.
Binford, L.R., 1986b. Reply to: Further comment on fauna from Klasies River mouth. Curr. Anthropol. 27, 512–515.
Blome, M.W., Cohen, A.S., Tryon, C.A., Brooks, A.S., Russell, J., 2012. The environmental context for the origins of modern human diversity: A synthesis of regional variability in african climate 150,000-30,000 years ago. J. Hum. Evol. 62, 563–592.
Bräuer, G., 1992. Africa's place in the evolution of *Homo sapiens*. In: Bräuer, G., Smith, F.H. (Eds.), Continuity or Replacement? Controversies in *Homo sapiens* Evolution. Balkema, Rotterdam, pp. 83–98.
Bräuer, G., Singer, R., 1996. The Klasies zygomatic bone: Archaic or modern? J. Hum. Evol. 30, 161–165.
Bräuer, G., Deacon, H.J., Zipfel, F., 1992. Comment on the new maxillary finds from Klasies River, South Africa. J. Hum. Evol. 23, 419–422.
Butzer, K.W., 1982. Geomorphology and sediment stratigraphy. In: Singer, R., Wymer, J. (Eds.), The Middle Stone Age at Klasies River Mouth in South Africa. Chicago University Press, Chicago, pp. 33–42.
Cameron, M.E., Pfeiffer, S., Stock, J., 2021. Small body size phenotypes among middle and later stone age southern africans. J. Hum. Evol. 152, 102943.
Canti, M.G., Brochier, J.E., 2017. Plant ash. In: Nicosia, C., Stoops, G. (Eds.), Archaeological Soil and Sediment Micromorphology. Wiley Blackwell, Hoboken, pp. 147–154.
Clark, A.E., Ranlett, S., Stiner, M.C., 2022. Domestic spaces as crucibles of Paleolithic culture: An archaeological perspective. J. Hum. Evol. 172, 103266.
Courty, M.A., 2001. Microfacies analysis assisting archaeological stratigraphy. In: Goldberg, P., Holliday, V.T., Ferring, C.F. (Eds.), Earth Sciences and Archaeology. Springer, Boston, pp. 205–239.
Deacon, H.J., 1993. Planting an idea: An archaeology of stone age gatherers in South Africa. S. Afr. Archaeol. Bull. 48, 86–93.
Deacon, H.J., 1995. Two late pleistocene-holocene archaeological depositories from the southern Cape, South Africa. S. Afr. Archaeol. Bull. 50, 121–131.
Deacon, H.J., 1998. Elandsfontein and Klasies River revisited. In: Ashton, N., Healy, F., Pettitt, P. (Eds.), Stone Age Archaeology: Essays in Honour of John Wymer. Oxbow Books, Oxford, pp. 23–28.
Deacon, H.J., 2008. The context of the 1967–8 sample of human remains from cave 1 Klasies River Main site. South Afr. Archaeol. Soc. Goodwin Ser. 10, 143–149.
Deacon, H.J., Geleijnse, V.B., 1988. The stratigraphy and sedimentology of the main site sequence, Klasies River, South Africa. S. Afr. Archaeol. Bull. 43, 5–14.
Deacon, H.J., Schuurman, R., 1992. The origins of modem people: The evidence from Klasies River. In: Bräuer, G., Smith, F.H. (Eds.), Continuity or Replacement: Controversies in *Homo sapiens* Evolution. Balkema, Rotterdam, pp. 121–129.
Deacon, H.J., Adams, B., Deacon, J., Geleijnse, V.B., Thackeray, A.I., Thackeray, J.F., Avery, D.M., Binneman, J.N.F., Brink, J.S., Goede, A., Loubser, G., Vogel, J.C., 1986. The Maintenance of Human Populations in the Late Pleistocene. Unpublished report to the Human Sciences Research Council.
Deacon, H.J., Talma, A.S., Vogel, J.C., 1988. Biological and cultural development of Pleistocene people in an Old World southern continent. In: Prescott, J.R. (Ed.), Early Man in the Southern Hemisphere. University of Adelaide, Adelaide, pp. 523–531.
Farrand, W.R., 2001. Sediments and stratigraphy in rockshelters and caves: A personal perspective on principles and pragmatics. Geoarchaeology 16, 537–557.

Feathers, J.K., 2002. Luminescence dating in less than ideal conditions: Case studies from Klasies River main site and Duinefontein, South Africa. J. Archaeol. Sci. 29, 177–194.
Frayer, D.W., Wolpoff, M.H., Thorne, A.G., Smith, F.H., Pope, G.G., 1993. Theories of modern human origins: The paleontological test. Am. Anthropol. 95, 14–50.
Glenn, C.R., Föllmi, K.F., Riggs, S.R., Baturin, G.N., Grimm, K.A., Trappe, J., Abed, A.M., Galli-Olivier, C., Garrison, R.E., Ilyin, A.I., Jehl, C., Rohrlich, V., Sadaqah, R.M.Y., Schidlowski, M., Sheldon, R.E., Siegmund, H., 1994. Phosphorus and phosphorites: Sedimentology and environments of formation. Eclogae Geol. Helv. 87, 747–788.
Goede, A., Hitchman, M.A., 1987. Electron spin resonance analysis of marine gastropods from coastal archaeological sites in southern Africa. Archaeometry 29, 163–174.
Goldberg, P., 2000. Micromorphology and site formation at Die Kelders cave I, South Africa. J. Hum. Evol. 38, 43–90.
Goldberg, P., Sherwood, S.C., 2006. Deciphering human prehistory through the Geoarchaeological study of cave sediments. Evol. Anthropol. 15, 20–36.
Goldberg, P., Miller, C., Schiegl, S., Ligouis, B., Berna, F., Conard, N., Wadley, L., 2009. Bedding, hearths, and site maintenance in the middle stone age of sibudu cave, KwaZulu-natal, South Africa. Archaeol. Anthropol. Sci. 1, 95–122.
Grine, F.E., 2000. Middle stone age human fossils from Die Kelders cave 1, western Cape province, South Africa. J. Hum. Evol. 38, 129–145.
Grine, F.E., 2016. The Late Quaternary hominins of Africa: The skeletal evidence from MIS 6–2. In: Jones, S.C., Stewart, B.A. (Eds.), Africa from MIS 6–2: Population Dynamics and Paleoenvironments. Springer, Dordrecht, pp. 323–381.
Grine, F.E., Pearson, O.M., Klein, R.G., Rightmire, G.P., 1998. Additional human fossils from Klasies River mouth, South Africa. J. Hum. Evol. 35, 95–107.
Grine, F.E., Marean, C.W., Faith, J.T., Black, W., Mongle, C.S., Trinkaus, E., le Roux, S.G., du Plessis, A., 2017a. Further human fossils from the middle stone age deposits of Die Kelders cave 1, western Cape province, South Africa. J. Hum. Evol. 109, 70–78.
Grine, F.E., Wurz, S., Marean, C.W., 2017b. The middle stone age human fossil record from Klasies River Main site. J. Hum. Evol. 103, 53–78.
Grine, F.E., Mongle, C.S., Smith, S.L., Black, W., du Plessis, A., Braga, J., 2020. Human manual distal phalanges from the middle stone age deposits of Klasies River Main site, western Cape province, South Africa. J. Hum. Evol. 146, 102849.
Grine, F.E., Gonzalvo, E., Rossouw, L., Holt, S., Black, W., Braga, J., 2021. Variation in Middle Stone Age mandibular molar enamel-dentine junction topography at Klasies River Main Site assessed by diffeomorphic surface matching. J. Hum. Evol. 161, 103079.
Grine, F.E., Mongle, C.S., Kollmer, W., Romanos, G., du Plessis, A., Maureille, B., Braga, J., 2023. Hypercementosis in late Pleistocene *Homo sapiens* fossils from Klasies River Main site, South Africa. Arch. Oral Biol. 149, 105664.
Haaland, M.M., Miller, C.E., Unhammer, O.F., Reynard, J.P., van Niekerk, K.L., Ligouis, B., Mentzer, S.M., Henshilwood, C.S., 2021. Geoarchaeological investigation of occupation deposits in Blombos Cave in South Africa indicate changes in site use and settlement dynamics in the southern Cape during MIS 5b-4. Quat. Res. 100, 170–223.
Henderson, Z., 1990. Aspects of the archaeology at Klasies River: A study of context and association in shelter 1B. Masters thesis, University of Stellenbosch.
Henderson, Z., 1992. The context of some Middle Stone Age hearths at Klasies River shelter 1b: Implications for understanding human behaviour. South. Afr. Field Archaeol. 1, 14–26.
Henshilwood, C.S., Marean, C.W., 2003. The origin of modern human behavior: Critique of the models and their test implications. Curr. Anthropol. 44, 627–651.
Henshilwood, C.S., d'Errico, F., Vanhaeren, M., van Niekerk, K., Jacobs, Z., 2004. Middle stone age shell beads from South Africa. Science 384, 404.
Henshilwood, C.S., d' Errico, F., Watts, I., 2009. Engraved ochres from the middle stone age levels at blombos cave, South Africa. J. Hum. Evol. 57, 27–47.
Henshilwood, C.S., d'Errico, F., Van Niekerk, K.L., Coquinot, Y., Jacobs, Z., Lauritzen, S.E., Menu, M., García-Moreno, R., 2011. A 100,000-year-old ochre-processing workshop at Blombos Cave, South Africa. Science 334, 219–222.
Holliday, V.T., Mandel, R.D., Bettis, E.A., 2017. Soils. In: Gilbert, A.S., Goldberg, P., Holliday, V.T., Mandel, R.D., Sternberg, R.S. (Eds.), Encyclopedia of Geoarchaeology. Springer, Dordrecht, pp. 862–877.
Jennings, J.E., Brink, A.B.A., 1961. A guide to soil profiling for civil engineering purposes in South Africa. Trans. S. Afr. Inst. Civ. Eng. 3, 145–151.
Karkanas, P., 2017. Guano. In: Nicosia, C., Stoops, G. (Eds.), Archaeological Soil and Sediment Micromorphology. Wiley Blackwell, Hoboken, pp. 83–90.
Karkanas, P., 2021. All about wood ash: Long term fire experiments reveal unknown aspects of the formation and preservation of ash with critical implications on the emergence and use of fire in the past. J. Archaeol. Sci. 135, 105476.
Karkanas, P., Goldberg, P., 2010. Site formation processes at pinnacle point cave 13B (Mossel bay, western Cape province, South Africa): Resolving stratigraphic and depositional complexities with micromorphology. J. Hum. Evol. 59, 256–273.
Karkanas, P., Bar-Yosef, O., Goldberg, P., Weiner, S., 2000. Diagenesis in prehistoric caves: The use of minerals that form in situ to assess the completeness of the archaeological record. J. Archaeol. Sci. 27, 915–929.
Karkanas, P., Shahack-Gross, R., Ayalon, A., Bar-Matthews, M., Barkai, R., Frumkin, A., Gopher, A., Stiner, M., 2007. Evidence for habitual use of fire at the end of the Lower Paleolithic: Site formation processes at Qesem Cave, Israel. J. Hum. Evol. 53, 197–212.
Karkanas, P., Brown, K.S., Fisher, E.C., Jacobs, Z., Marean, C.W., 2015. Interpreting human behavior from depositional rates and combustion features through the study of sedimentary microfacies at site Pinnacle Point 5–6, South Africa. J. Hum. Evol. 85, 1–21.
Klein, R.G., 1976. The mammalian fauna of the Klasies River mouth sites, southern Cape province, South Africa. S. Afr. Archaeol. Bull. 31, 75–98.
Lam, Y.M., Pearson, O.M., Smith, C.M., 1996. Chin morphology and sexual dimorphism in the fossil hominid mandible sample from Klasies River Mouth. Am. J. Phys. Anthropol. 100, 545–557.
Larbey, C., Mentzer, S.M., Ligouis, B., Wurz, S., Jones, M.K., 2019. Cooked starchy food in hearths ca. 120 kya and 65 kya (MIS 5e and MIS 4) from Klasies River Cave, South Africa. J. Hum. Evol. 131, 210–227.
Loftus, E., Sealy, J., Leng, M.J., Lee-Thorp, J.A., 2017. A late Quaternary record of seasonal sea surface temperatures off southern Africa. Quat. Sci. Rev. 171, 73–84.
Mallol, C., Goldberg, P., 2017. Cave and rockshelter sediments. In: Nicosia, C., Stoops, G. (Eds.), Archaeological Soil and Sediment Micromorphology. Wiley Blackwell, Hoboken, pp. 359–382.
Mallol, C., Mentzer, S.M., 2017. Contacts under the lens: Perspectives on the role of microstratigraphy in archaeological research. Archaeol. Anthropol. Sci. 9, 1645–1669.
Mallol, C., Hernández, C.M., Cabanes, D., Machado, J., Sistiaga, A., Pérez, L., Galván, B., 2013a. Human actions performed on simple combustion structures: An experimental approach to the study of Middle Palaeolithic fire. Quat. Int. 315, 3–15.
Mallol, C., Hernández, C.M., Cabanes, D., Sistiaga, A., Machado, J., Rodríguez, Á., Pérez, L., Galván, B., 2013b. The black layer of Middle Palaeolithic combustion structures. Interpretation and archaeostratigraphic implications. J. Archaeol. Sci. 40, 2515–2537.
Mallol, C., Mentzer, S.M., Miller, C.E., 2017. Combustion features. In: Nicosia, C., Stoops, G. (Eds.), Archaeological Soil and Sediment Micromorphology. Wiley Blackwell, Hoboken, pp. 299–330.
Marean, C.W., 2014. The origins and significance of coastal resource use in Africa and Western Eurasia. J. Hum. Evol. 77, 17–40.
Marean, C.W., 2016. The transition to foraging for dense and predictable resources and its impact on the evolution of modern humans. Philos. Trans. R. Soc. B Biol. Sci. 371, 20150239.
Marean, C.W., Bar-Matthews, M., Bernatchez, J.A., Fisher, E.C., Goldberg, P., Herries, A.I.R., Jacobs, Z., Jerardino, A., Karkanas, P., Minichillo, T., Nilssen, P.J., Thompson, E., Watts, I., Williams, H.M., 2007. Early human use of marine resources and pigment in South Africa during the Middle Pleistocene. Nature 449, 906–909.
McBrearty, S., Brooks, A., 2000. The revolution that wasn't: A new interpretation of the origin of modern human behavior. J. Hum. Evol. 39, 453–563.
Mentzer, S.M., 2014. Microarchaeological approaches to the identification and interpretation of combustion features in prehistoric archaeological sites. J. Archaeol. Method Theor 21, 616–668.
Mentzer, S.M., 2017. Micro XRF. In: Nicosia, C., Stoops, G. (Eds.), Archaeological Soil and Sediment Micromorphology. Wiley Blackwell, Hoboken, pp. 431–440.
Mentzer, S., Placzek, C., Miller, C.E., Wurz, S., July 2014. New geoarchaeological analyses at Klasies River main site, Cave 1. 14th Congress of the Pan African Archaeological Association for Prehistory and Related Studies and the 22nd Biennial Meeting of the Society of Africanist Archaeologists, 2014, pp. 14–18.
Miller, C.E., Conard, N.J., Goldberg, P., Berna, F., 2010. Dumping, sweeping and trampling: Experimental micromorphological analysis of anthropogenically modified combustion features. Palethnologie 25–37.
Miller, C.E., Goldberg, P., Berna, F., 2013. Geoarchaeological investigations at Diepkloof rock shelter, western Cape, South Africa. J. Archaeol. Sci. 40, 3432–3452.
Miller, C.E., Mentzer, S.M., Berthold, C., Leach, P., Ligouis, B., Tribolo, C., Parkington, J., Porraz, G., 2016. Site-formation processes at elands bay cave, South Africa. South. Afr. Humanit 29, 69–128.
Miller, G.H., Beaumont, P.B., Deacon, H.J., Brooks, A.S., Hare, P.E., Jull, A.J.T., 1999. Earliest modern humans in southern Africa dated by isoleucine epimerization in ostrich eggshell. Quat. Sci. Rev. 18, 1537–1548.
Moini, M., Rollman, C.M., France, C.A., 2013. Dating human bone: Is racemization dating species-specific? Anal. Chem. 85, 11211–11215.
Morrissey, P., Mentzer, S.M., Wurz, S., 2022. A critical review of the stratigraphic context of the MSA I and II at Klasies River Main site, South Africa. J. Paleolit. Archaeol. 5, 5.
Niespolo, E.M., Sharp, W.D., Avery, G., Dawson, T.E., 2021. Early, intensive marine resource exploitation by Middle Stone Age humans at Ysterfontein 1 rockshelter, South Africa. Proc. Natl. Acad. Sci. USA 118, e2020042118.
Rentzel, P., Nicosia, C., Gebhardt, A., Brönnimann, D., Pümpin, C., Ismail-Meyer, K., 2017. Trampling, poaching and the effect of traffic. In: Nicosia, C., Stoops, G. (Eds.), Archaeological Soil and Sediment Micromorphology. Wiley Blackwell, Hoboken, pp. 281–297.
Reynard, J.P., 2021. Paradise lost: Large mammal remains as a proxy for environmental change from MIS 6 to the Holocene in southern Africa. S. Afr. J. Geol. 124, 1055–1072.
Reynard, J.P., Wurz, S., 2020. The palaeoecology of Klasies River, South Africa: An analysis of the large mammal remains from the 1984–1995 excavations of Cave 1 and 1A. Quat. Sci. Rev. 237, 106301.
Rightmire, G.P., 2009. Middle and later Pleistocene hominins in Africa and southwest asia. Proc. Natl. Acad. Sci. USA 106, 16046–16050.
Rightmire, G.P., Deacon, H.J., 1991. Comparative studies of late Pleistocene human remains from Klasies River mouth, South Africa. J. Hum. Evol. 20, 131–156.
Rightmire, G.P., Deacon, H.J., 2001. New human teeth from the middle stone age deposits at Klasies River, South Africa. J. Hum. Evol. 41, 535–544.

Rightmire, G.P., Deacon, H.J., Schwartz, J.H., Tattersall, I., 2006. Human foot bones from Klasies River main site, South Africa. J. Hum. Evol. 50, 96–103.
Roebroeks, W., Villa, P., 2011. On the earliest evidence for habitual use of fire in Europe. Proc. Natl. Acad. Sci. USA 108, 5209–5214.
Royer, D.F., Lockwood, C.A., Scott, J.E., Grine, F.E., 2009. Size variation in early human mandibles and molars from Klasies River, South Africa: Comparison with other Middle and Late Pleistocene assemblages and with modern humans. Am. J. Phys. Anthropol. 140, 312–323.
Schiegl, S., Goldberg, P., Bar-Yosef, O., Weiner, S., 1996. Ash deposits in Hayonim and Kebara Caves, Israel: Macroscopic, microscopic and mineralogical observations, and their archaeological implications. J. Archaeol. Sci. 23, 763–781.
Shackleton, N.J., 1982. Stratigraphy and chronology of the Klasies River mouth deposits: Oxygen isotope evidence. In: Singer, R., Wymer, J. (Eds.), The Middle Stone Age at Klasies River Mouth in South Africa. University of Chicago Press, Chicago, pp. 194–199.
Singer, R., Wymer, J., 1982. The Middle Stone Age at Klasies River Mouth in South Africa. Chicago University Press, Chicago.
Singer, R., Wymer, J., 1986. On Binford on Klasies River mouth: Response of the excavators. Curr. Anthropol. 27, 56–57.
Smith, F.H., 1992. Models and realities in modern human origins: The African fossil evidence. Philos. Trans. R. Soc. B Biol. Sci. 337, 243–250.
Stoops, G., 2021. Guidelines for Analysis and Description of Soil and Regolith Thin Sections, Second Edition. Wiley, Hoboken.
Thackeray, A.I., 1989. Changing fashions in the Middle Stone Age: The stone artifact sequence from Klasies River main site, South Africa. Afr. Archaeol. Rev. 7, 33–57.
Thackeray, A.I., 1992. The middle stone age south of the Limpopo River. J. World Prehist. 6, 385–440.
Thackeray, J.F., 1986. Further comment on fauna from Klasies River mouth. Curr. Anthropol. 27, 511.
Thackeray, J.F., 2018. Oxygen isotope ratios of Turbo sarmaticus molluscan opercula from Late Pleistocene archaeological deposits, Klasies River, South Africa. S. Afr. Archaeol. Bull. 73, 143–146.
Tribolo, C., Mercier, N., Martin, L., Taffin, N., Miller, C.E., Will, M., Conard, N., 2022. Luminescence dating estimates for the coastal MSA sequence of Hoedjiespunt 1 (South Africa). J. Archaeol. Sci. Rep. 41, 103320.
Van Pletzen-Vos, L., Brink, J., Reynard, J.P., Wurz, S., 2019. Revisiting Klasies River: A report on the large mammal remains from the Deacon excavations of Klasies River Main site, South Africa. S. Afr. Archaeol. Bull. 74, 127–137.
Villagran, X.S., 2019. The shell midden conundrum: Comparative micromorphology of shell-matrix sites from South America. J. Archaeol. Method Theor 26, 344–395.
Villagran, X.S., Balbo, A.L., Madella, M., Vila, A., Estevez, J., 2011. Stratigraphic and spatial variability in shell middens: Microfacies identification at the ethnohistoric site Tunel VII (Tierra del Fuego, Argentina). Archaeol. Anthropol. Sci. 3, 357–378.
Vogel, J.C., 2001. Radiometric dates for the middle stone age in South Africa. In: Tobias, P.V., Raath, M.A., Moggi-Cecchi, J., Doyle, G.A. (Eds.), Humanity from African Naissance to Coming Millennia-Colloquia in Human Biology and Palaeoanthropology. Florence University Press, Florence, pp. 261–268.
Wadley, L., 2015. Those marvellous millennia: The middle stone age of southern Africa. Azania 50, 155–226.
Wadley, L., Sievers, C., Bamford, M., Goldberg, P., Berna, F., Miller, C., 2011. Middle Stone Age bedding construction and settlement patterns at Sibudu, South Africa. Science 334, 1388–1391.
Wadley, L., Esteban, I., De La Peña, P., Wojcieszak, M., Stratford, D., Lennox, S., d'Errico, F., Rosso, D.E., Orange, F., Backwell, L., Sievers, C., 2020. Fire and grass-bedding construction 200 thousand years ago at Border Cave, South Africa. Science 369, 863–866.
Weiner, S., Goldberg, P., Bar-Yosef, O., 2002. Three-dimensional distribution of minerals in the sediments of Hayonim Cave, Israel: Diagenetic processes and archaeological implications. J. Archaeol. Sci. 29, 1289–1308.
Wolpoff, M.H., Caspari, R., 1996. The modernity mess. J. Hum. Evol. 30, 167–172.
Wurz, S., 2002. Variability in the middle stone age lithic sequence, 115 000–60 000 years ago at Klasies River, South Africa. J. Archaeol. Sci. 29, 1001–1015.
Wurz, S., Bentsen, S., Reynard, J., Van Pletzen-Vos, L., Brenner, M., Mentzer, S., Pickering, R., Green, H.E., 2018. Connections, culture and environments 100,000 years ago at Klasies River main site. Quat. Int. 495, 102–115.
Wurz, S., Pickering, R., Mentzer, S.M., 2022. U-Th dating, taphonomy, and taxonomy of shell middens at Klasies River main site indicate stable and systematic coastal exploitation by MIS 5c-d. Front. Earth Sci. 10, 1001370.